Developments in compartmentalized bimetallic transition metal ethylene polymerization catalysts

Hongyi Suo,[a,b] Gregory A. Solan,*[a,c] Yanping Ma,[a] and Wen-Hua Sun*[a,b,d]

[a] Key Laboratory of Engineering Plastics and Beijing National Laboratory for Molecular Science, Institute of Chemistry, Chinese Academy of Sciences, Beijing 100190, China.

[b] CAS Research/Education Center for Excellence in Molecular Sciences, University of Chinese Academy of Sciences, Beijing 100049, China.

[c] Department of Chemistry, University of Leicester, University Road, Leicester LE1 7RH, UK.

[d] State Key Laboratory for Oxo Synthesis and Selective Oxidation, Lanzhou Institute of Chemical Physics, Chinese Academy of Sciences, Lanzhou 730000, China.

Contents

Graphic Abstract

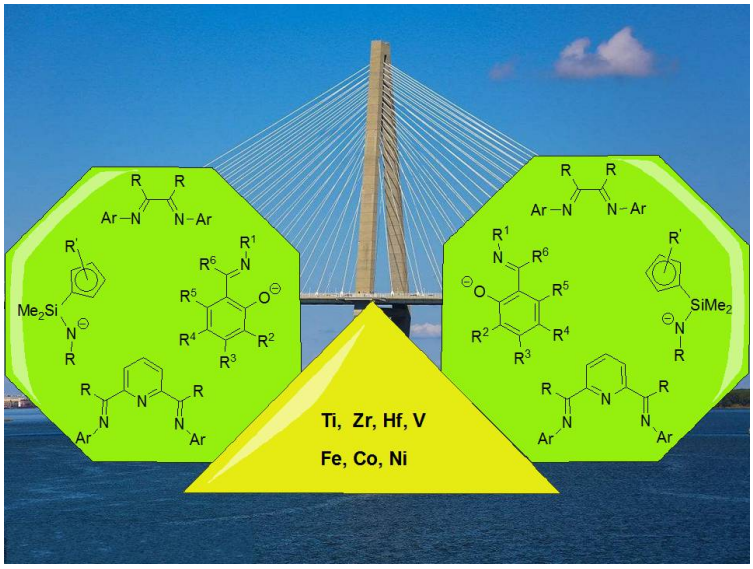

Abstract

Recent progress concerning the application of compartmentalized bimetallic complexes as homogeneous catalysts in ethylene polymerization is reviewed with particular regard to metal-metal combinations based on either early- (Ti, Zr, Hf and V) or late-transition metals (Fe, Co and Ni). The effect of positioning two polymerization-active metal centers in close proximity on catalytic activity, molecular weight, molecular weight distribution and levels of branching are thoroughly documented. Compartmental ligands comprising binding domains consisting of phenoxyimines, *ansa*-bridged cyclopentadienyl-amides, α-diimines and iminopyridines are described as is their capacity to serve as compatible binucleating supports for homobimetallic and also for the less investigated heterobimetallic counterparts. By comparison with their mononuclear analogs, any synergic properties exhibited by these binuclear catalysts represents an underlying theme to be developed where possible throughout this review.

Keywords: Bimetallic complex; Early transition metal; Late transition metal; Catalyst; Compartmental ligand; Ethylene polymerization; Polyethylene microstructure.

1. Introduction

The metal-mediated conversion of cheap olefinic monomers (*e.g.*, ethylene, propylene, α-olefins) to highly versatile polyolefinic materials is a field of research with a long and distinguished track record. Variations in the particular metal catalyst employed can have dramatic effects on the polymerization process leading to a plethora of important polymers with far reaching uses in the materials industry [1]. Among the types of homogeneous catalyst employed, the bulk of the research effort over the

years has been dedicated to the study of systems based on a single metal center drawn from the transition metal series. Indeed, this type of catalyst has been the subject of many excellent reviews, some of the more recent examples being referenced herein [2-5]. With regard to late transition metal catalysts for ethylene polymerization, numerous studies have been directed towards modifying the classic bis(imino)pyridine supporting ligand by changing the substituents of the imino-linked N-aryl moieties [6, 7] as well as the substituents on the imine-carbon atom [8, 9] [10-12]. One major breakthrough was establishing that sterically bulky groups tend to promote polymer chain growth over chain transfer by blocking coordination sites on the metal complexes [13, 14].

As an emerging strategy within the polymerization arena, the bimetallic approach in which two polymerization-active metal centers are compartmentalized on the same ligand framework, has been attracting growing attention. This can, in part, be attributed to the promising cooperative effects [15, 16] imparted by the close proximity of the two metal centers which is not achievable with a mononuclear catalyst. Indeed, bimetallic olefin polymerization catalysts can exhibit remarkable synergic effects in catalytic activity, polymer microstructure (*e.g.*, molecular weight, chain branching, monomer repeat regioregularity) as well as selectivity for co-monomer enchainment [1]. Several examples have now been disclosed suggesting the importance of cooperativity between metallic sites in the development of new catalysts [17-19].

In the late 1990s, it was shown that certain phenoxyimine compounds (**I** in Chart 1) could serve as compatible ligands for both early and late transition metal olefin polymerization catalysts. In particular, the so-called FI-group IV catalysts, when suitably activated, exhibit unprecedented catalytic activities for the polymerization of ethylene [20, 21]. Meanwhile, phenoxyimine-nickel complexes have displayed not only high catalytic activity but also good functional group tolerance [16]. By providing a suitable steric environment around the nickel center through the introduction of strategically placed substituents on **I**, chain transfer reactions via β-H elimination can be suppressed leading to the production of high molecular weight polymers [13].

Elsewhere, complexes containing a cyclopentadienyl-silyl-amido ligand scaffold (**II** in Chart 1), later named constrained geometry catalysts (CGCs), have proved industrially relevant catalysts based on early transition metals [22]. Importantly, polymerizations with these species can be carried out at high reactor temperatures when activated with the appropriate co-catalyst [23]. They can be described as efficient ethylene polymerization catalysts with high polymerization activities and the unusual capacity to enchain bulky co-monomers, which reflects the sterically open, coordinately unsaturated architectures. Moreover, high molecular weight polymers can be obtained due to the relatively slow rates of chain transfer [1].

Late transition metal catalysts bearing numerous types of neutral imine-based N,N,N and N,N ligands have been well documented since their emergence in the mid

to late 1990s. Indeed, the prototypical bis(arylimino)pyridine (**III**, Chart 1) and α-diimine (**IV**, Chart 1) remain the benchmarks and continue to be the source of new developments. Indeed, examples of iron and cobalt catalysts bearing **III** have now emerged that not only exhibit exceptional performance and high thermal stabilities but are also capable of promoting a broad range of oligomer and polymer properties [12, 24, 25]. Furthermore, these types of catalyst can produce polymers incorporating a range of branching contents [11, 26].

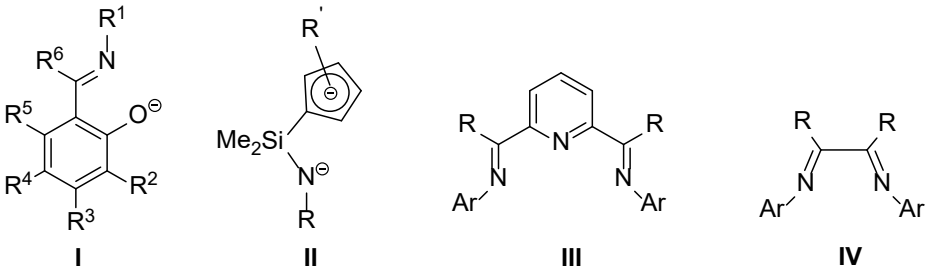

Chart 1 The four main types of chelating ligand highlighted in this review.

In this review, we are concerned with binuclear early and late transition metal complexes that incorporate binding domains based on mainly the chelation pockets found in **I** – **IV** (Chart 1). Considerable effort will be made to correlate effects of catalyst structure on polymerization activity, molecular weight, molecular weight distribution and branching content. In addition, any cooperative effects imparted by the presence of the two closely located metal centers will be fully discussed.

2. Binuclear early transition metal catalysts for ethylene homo- and copolymerization

Homobimetallic group 4 catalysts based on phenoxyimine [27, 28] and cyclopentadienyl-silyl-amido ligands (Ti_2 [29-31] , Zr_2 [19, 32, 33]), have been shown to exhibit distinctive cooperative effects by producing polyolefins with substantially higher molecular weights when compared to their corresponding monometallic analogues. In addition, heterobimetallic systems (TiZr, [34] TiCr [35, 36]) based on cyclopentadienyl-silyl-amido ligands have also been reported (*vide infra*).

Phenoxyimine catalysts demonstrate excellent performance in terms of both catalytic activity and stereocontrol in olefin polymerization [37]. Ma's group has synthesized the binuclear hetero-ligated titanium catalysts (**1** and **2**, Fig. 1) for ethylene polymerization and copolymerization [37]. The molecular structure of **1** shows that this bimetallic molecule possesses a tweezer-like structure exhibiting C_2 symmetry with the distance between the two titanium atoms being 7.88 Å, which suggests significant repulsive interactions between the two catalytic sites. The catalytic activity of **1** can reach up to 2.95×10^6 g mol^{-1} h^{-1} with the polymer displaying a narrow PDI of 1.71 and a M_w of up to 1.7×10^2 kg mol^{-1}. In comparison, its mononuclear counterpart exhibited slightly higher activity (3.12×10^6 g mol^{-1} h^{-1})

with a narrower PDI (1.66) along with higher M_w (1.9×10^2 kg mol^{-1}). On the other hand, **2** though displaying quite low activity, showed superior results in terms of activity, PDI and molecular weight when compared with its mononuclear counterpart (activity: 1.6×10^4 g mol^{-1} h^{-1} *vs.* 0.6×10^4 g mol^{-1} h^{-1}, PDI: 3.26 *vs.* 49.3 and M_w: 6.4 $\times 10^2$ kg mol^{-1} *vs.* 5.1×10^2 kg mol^{-1}). In addition, both **1** and **2** can copolymerize ethylene with monoenes and dienes.

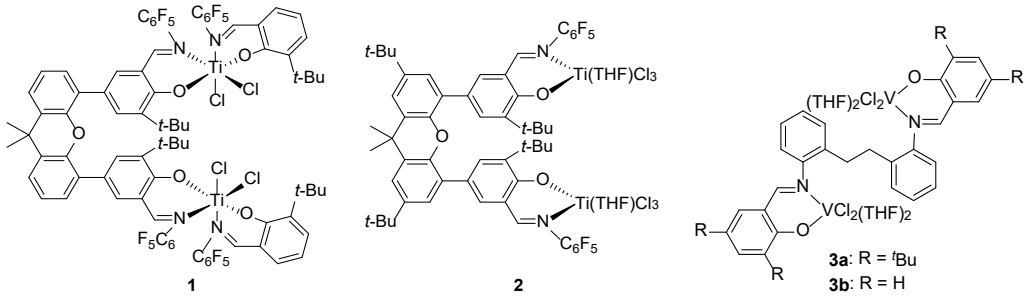

Fig. 1 Bis(phenoxyimine) catalysts based on titanium and vanadium.

In the last few years, highly active bimetallic catalysts based on group 5 metals have for the first time appeared in the academic literature [38-40]. These complexes have tended to be designed around the phenoxyimine ligand frame with divanadium precatalysts, **3a** and **3b** (Fig. 1) providing two notable examples. Indeed, **3a** and **3b** have been used to polymerize ethylene on activation with ethyl trichloroacetate (ETA) and dimethylaluminum chloride (DMAC) [41]. The performance of *tert*-butyl-substituted **3a** proved a more potent catalyst, as evidenced by the two times higher activity (9.52×10^6 g mol^{-1} h^{-1} (**3a**) *vs.* 4.80×10^6 g mol^{-1} h^{-1} (**3b**)), almost three times higher molecular weight (M_w: 445 kg mol^{-1} (**3a**) *vs* 1.70 kg mol^{-1} (**3b**)) and narrower PDI (2.5 (**3a**) *vs.* 5.6 (**3b**)). Furthermore, it was evident that the activities for the bimetallic systems were somewhat higher than their monometallic analogues, with the M_w value of the polyethylene obtained using **3b** was at the lower end of those measured. In addition, both catalysts showed they were active for the polymerization of ε-caprolactone.

Monometallic constrained geometry catalysts have been well-studied as ethylene polymerization catalysts typically displaying high activities and forming high molecular weight polymer; observations that highlight their relatively slow rates of chain-transfer. Group 4 metals are widely employed in mononuclear CGC catalysts with polymerization activity falling approximately in the order Ti > Zr > Hf [1]. The molecular structures of **4c** and **4d** reveal significant differences in the Zr···Zr distances between the methylene- and ethylene-bridged complexes (Fig. 2) [33, 42]. In methylene-bridged **4c**, the Zr···Zr distance of 7.06 Å can be attributed to the large indenyl-CH_2-indenyl rotational barrier (~65 kcal/mol), while the ethylene-bridged **4d** has a negligible rotational barrier which results in a distance of 8.67 Å. On activation with MAO, both **4a** and **4b** gave similar activities (2.5×10^4 g mol^{-1} h^{-1} *vs.* 2.3×10^4 g mol^{-1} h^{-1}) and high molecular weight polyethylene (M_n: 244 kg mol^{-1} *vs.* 268 kg mol^{-1})

with no evidence of ethyl branches, which is almost 300 times that observed for the mono-zirconium catalyst (0.95 kg mol^{-1}) [1]. However, when **4c** and **4d** were activated by a bis-borate, the polymer formed displayed ethyl branches ranging from 1.3 to 12 per 1000 Cs and higher activities [8.7 × 10^4 g mol^{-1} h^{-1} (**4d**)]. This homopolymerization result suggests that the Zr···Zr spatial proximity significantly influences the rates of chain transfer. Their structurally related titanium complexes have also been used in copolymerization. As an additional feature, the polyethylenes produced by these bimetallic catalysts have significantly greater branching, with a predilection for ethyl branching, indicating favorable chain transfer to monomer, followed by α-olefin/polymer re-insertion (Scheme 1). The largest cooperative enchainment effects, when compared with the mononuclear controls, are achieved with the diborate-activated catalysts.

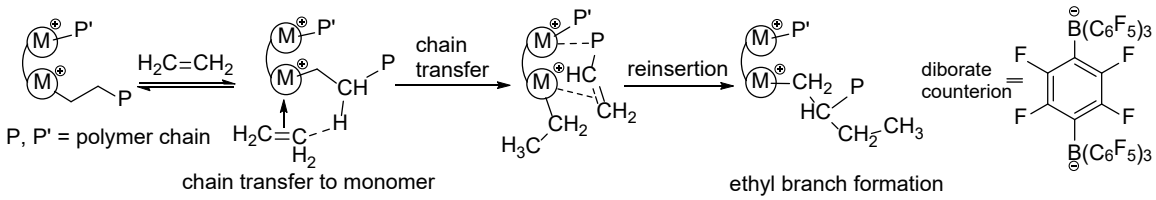

Scheme 1 Plausible mechanism for ethylene polymerization at a bimetallic CGC-Zr center.

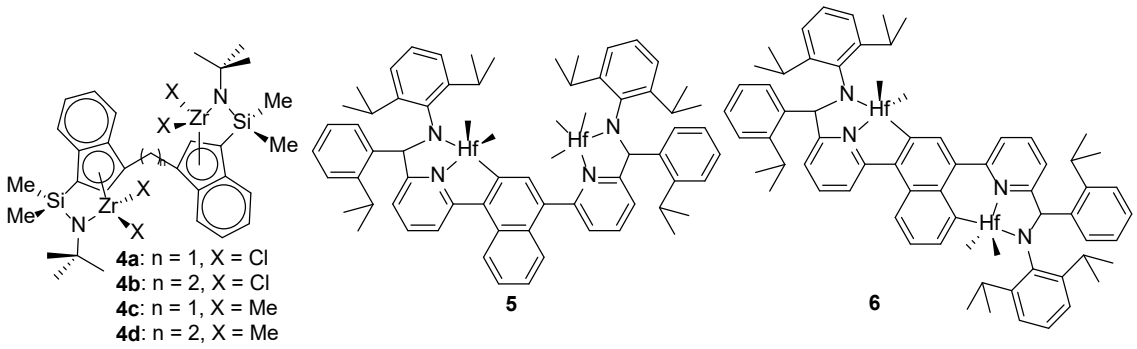

Fig. 2 Dizirconium and dihafnium constrained geometry-type precatalysts, **4** - **6**.

When compared with the multitude of polymerization studies focused on titanium and zirconium, hafnocene-based olefin polymerization catalysts have historically exhibited lower polymerization activities though producing higher M_w polyolefins [23, 43, 44]. Nonetheless, the dihafnium catalyst **5** (Fig. 2) exhibits pronounced bimetallic cooperative effects in ethylene homopolymerization, and indeed **6** (Fig. 2) produced polyethylene with 5.7 times higher M_w than its monometallic counterpart. Notably, in the solid state, the Hf···Hf distance is significantly different in **5** *vs*. **6** (6.16 *vs.* 8.06 Å, respectively) [45].

3. Binuclear late transition metal catalysts for ethylene homo- and co-polymerization

Late transition-metal (Fe, Co, Ni) olefin polymerization catalysts have attracted a lot

interest over the last twenty years or so due, in some measure, to their greater tolerance to polar monomers when compared with early transition-metal catalysts [13, 46]. The properties of these systems have been modified by a variety of design strategies including steric and electronic effects [8, 47-50], fluorine bonding [51, 52] and secondary metal ion effects [13, 53]. Moreover, the polymer properties are also influenced by the distance between the metal centers in bimetallic catalysts. In addition, the effects of additives on the olefin polymerization using dinuclear complexes have also been investigated [54-56].

3.1 Binuclear nickel catalysts

Nickel catalysts are capable of generating high molecular weight polyethylene with activities comparable to many early transition metal catalysts, while palladium catalysts can copolymerize olefins with polar monomers such as alkyl acrylates or methyl vinyl ketone [57]. There are two important types of chelating ligand used to support the metal center namely phenoxyimine (N,O) and α-diimine (N,N), both of which have been adapted for use as efficient frameworks in binuclear nickel complexes. In addition, a notable feature of the phenoxyimine-nickel complexes is that they are neutrally charged in their activated forms and therefore considered to possess even greater tolerance toward polar functional groups than the α-diimine-nickel complexes, which form cationic species upon activation [16].

3.1.1 Neutral bimetallic phenoxyimine-nickel catalysts

Binuclear phenoxyiminato-nickel catalysts have been shown to possess enhanced stability, activity, comonomer incorporation as well as greater tolerance for polar monomers in olefin polymerization when compared to related mononuclear catalysts [13]. Marks and co-workers synthesized a planar dinickel complex, supported by an aromatic bis(phenoxyiminato) ligand (**A** in Scheme 2) [58-60]. These catalysts exhibit notable cooperativity effects manifested by enhanced polymerization activity, more methyl chain branching and increased molecular weight. In addition, catalysts, composed of two nickel phenoxyimines and a linker (L), have been reported independently by several research groups including **B** and **C** (Scheme 2) [54, 61-66]. Notably, nickel catalysts based on macrocyclic **C**, reported by Lee and co-workers, displayed moderate catalytic activity for ethylene polymerization [67, 68].

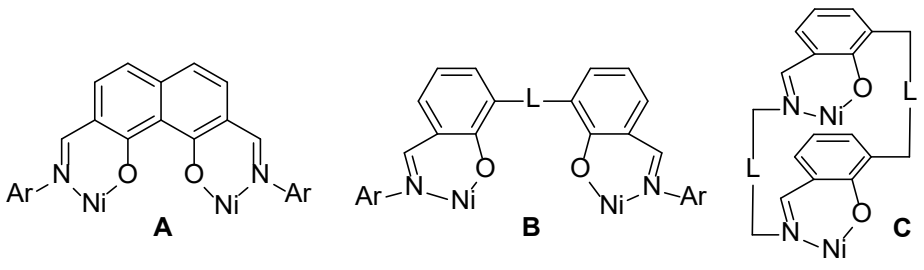

Scheme 2 Three general core structures of some dinuclear phenoxyimine-nickel complexes employed in olefin polymerization (L = linker).

Based on core **A** (Scheme 2), Marks and his group communicated the synthesis of binuclear naphthyloxydiiminato-nickel catalysts **7**, **8** (Fig. 3) and **9** (Fig. 4), in which the rigid binding ensures that the metal centers are held in close spatial proximity. Binuclear 2,7-diimino-1,8-dioxynaphthalene-nickel complexes **7a** and **7b** displaying Ni···Ni distances as small as ~3.1 Å, has seen their use as ethylene polymerization and copolymerization catalysts [58, 59]. Upon addition of $Ni(COD)_2$ (COD = 1,5-cyclooctadiene), **7a** and **7b** showed similar activities with polydispersities consistent with single-site species in ethylene polymerization. Notably, catalytic activities are almost six times higher than their mononuclear analogues. Furthermore, these binuclear catalysts produce highly branched polyethylenes (102 for **7a** and 105 for **7b**) in the absence of a co-catalyst.

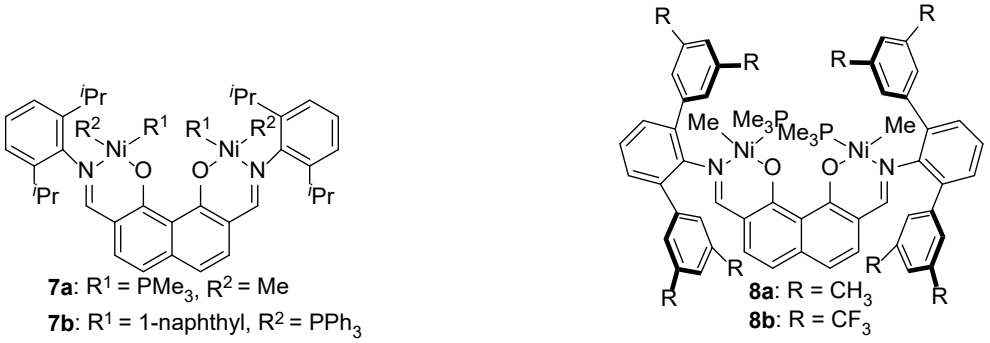

Fig. 3 Bimetallic nickel(II) precatalysts **7** and **8**

In addition, the use of **7** resulted in significantly more alkyl branches (*ca.* 90/1000 Cs) than the mononuclear catalysts (*ca.* 50/1000 Cs) and exhibited a strong selectivity for methyl-only branch formation (> 99%) [59]. Indeed, this enhanced activity is maintained in the presence of polar co-solvents. These results are in agreement with substantial Ni···Ni mediated cooperative effects in the enchainment process as shown by NMR spectroscopy. Indeed, a short Ni···Ni distance of 2.992(9) Å was apparent in the molecular structure which is shorter than the sum of the Ni atomic van der Waals radii (3.3 Å) and may allow chemically significant interactions [69]. In the presence of a polar co-solvent, the polymerization activities reduce in the order: toluene > diethyl ether > acetone > water. From the low temperature NMR spectroscopic studies, binuclear agostic interactions have been suggested and it is conceivable that secondary agostic binding as in structure **D** (Scheme 3) may influence the β-H elimination/re-insertion kinetics of the chain-walking processes. This increase in the propagation kinetics may reflect the monomer binding to the neighboring nickel center, thereby increasing the local concentrations [70].

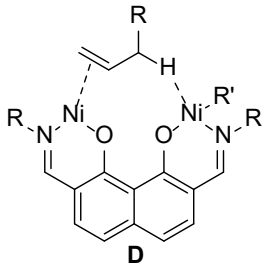

Scheme 3 A conceivable secondary agostic binding in structure **D**

However, when **7** is heated to 40 ºC, significant thermal deactivation takes place, forming a catalytically inactive bis-ligated species (Scheme 4) [58-60]. Therefore, in order to enhance the stability of the catalyst, bulkier substituted **8** were designed and synthesized (Fig. 3) [60]. According to the data listed in Table 1, the activity of **8** at 50 ºC increased nearly 4-fold when compared with **7**, with **8a** displaying the lowest M_w and **8b** the highest. Moreover, less methyl branches were observed using **8b**, which may be attributed to the short Ni···Ni distance of 5.8024(5) Å. At room temperature, **8a** and **8b** exhibited higher activity than that seen with the previously reported precatalyst **7** [58]. However, ethylene polymerizations mediated by monometallic analogues were significantly more rapid (72.8 and 200 × 10^4 g mol(Ni)$^{-1}$ h^{-1}). In general, the microstructures of the polyethylenes produced by these catalysts vary greatly depending on the N-terphenyl substitution. Furthermore, the methyl branching observed by **8a** (98/1000 Cs) and **8b** (47/1000 Cs) is higher than its mononuclear analogues (ranging from 7 − 91/1000 Cs), which may be due to Ni···Ni cooperative effects.

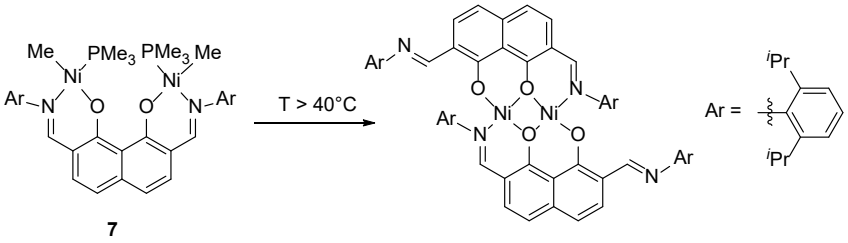

Scheme 4 Proposed thermal deactivation pathway of bimetallic catalyst **7**

Table 1 Catalytic and polymer properties displayed by **7** and **8**

Precat.	Co-cat.	T/ºC	t/min	Activity[a]	M_w[b]	M_w/M_n[b]	T_m[c]/ºC	Branches[d]
7a[e]	Ni(COD)$_2$	25	40	4.97	10.3	2.6	68	80
7b[e]	Ni(COD)$_2$	25	40	5.18	10.1	2.6	66	93
8a[f]	Ni(COD)$_2$	50	10	21.6	1.8	1.7	[g]	98
8b[f]	Ni(COD)$_2$	50	10	17.6	11	2.9	[g]	47
8a[f]	Ni(COD)$_2$	25	10	7.2	3.8	2.0	[g]	91
8b[f]	Ni(COD)$_2$	25	10	16.8	25	2.4	[g]	40

[a] Activity: × 10^4 g mol(Ni)$^{-1}$ h^{-1}.

[b] M_w in kg mol^{-1}. M_w and M_w/M_n determined by GPC.

[c] Determined by DSC.

[d] By ^{1}H NMR spectroscopy; expressed per 1000 Cs

[e] Polymerizations carried out with 10 μmol of catalyst and 2 equiv of co-catalyst/Ni in 25 mL of toluene at 7 atm of ethylene.

[f] Polymerizations carried out with 5.0 mmol catalyst and 2.0 equiv of co-catalyst/Ni in 50 mL toluene at 8 atm of ethylene.

[g] Not measured.

The structurally related **9** (Fig. 4), however, converted ethylene to semicrystalline polyethylene with a low degree of branching (*ca*. 10 branches/1000 Cs) [71]. The reduced number of branches suggests that binuclear nickel catalysts with a co-facial orientation and close proximity favor ethylene insertion into the Ni−C bond more significantly than their mononuclear analogues [13, 68].

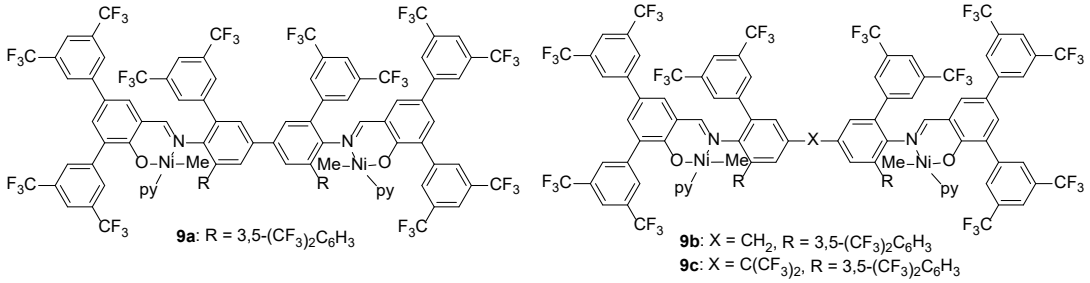

Fig. 4 Phenoxyimine-containing binuclear nickel complexes **9**

In the catalyst type **B** (Scheme 2), different catalytic properties for the binuclear nickel catalyst can be achieved by changing the structure of the linker, including the inclusion of aryl and alkyl groups (Fig. 5). The mononuclear counterparts of **10** showed low catalytic activity towards ethylene polymerization even when $Ni(COD)_2$ or $B(C_6F_5)_3$ was used as a phosphine acceptor [46]. However, binuclear **10** gave high activity up to 4.55×10^5 g mol(Ni)$^{-1}$ h^{-1} without the need for any co-catalyst (conditions: 10 μmol **10**, 43 ºC, 60 min, 21 atm ethylene pressure), forming polymer with a high M_w of up to 487.7 kg mol^{-1}. It is plausible that two separate nickel units act as mutually bulky *ortho*-substituted steric groups, which leads to the excellent catalytic performance. According to the ^{1}H NMR data, the average branching content of the polyethylenes is around 10 − 15 branches per 1000 Cs.

On activation with MAO, **11a** showed high activity, 3.76×10^5 g mol(Ni)$^{-1}$ h^{-1}, for ethylene polymerization [conditions: 3.41 μmol **11a**, 2000 of Al/Ni, 25 ºC, 30 min, 1 atm], producing polymer with a high M_w of 440 kg mol^{-1} while **11b** was inactive (Fig. 5) [62]. The activity increased with elevated temperature reaching 6.71×10^5 g mol(Ni)$^{-1}$ h^{-1} at 50 ºC; due to its poor solubility, the molecular weight was not determined. Substituting the linker in **11** for a methylene group, **12** were studied as single-component catalysts for ethylene polymerization [66]. The maximum activities

observed are significantly higher for the binuclear complexes [**12a**: 1.54 × 10^6 g mol(Ni)$^{-1}$ h^{-1} and **12b**: 1.15 × 10^6 g mol(Ni)$^{-1}$ h^{-1} *vs.* 2.1 × 10^5 g mol(Ni)$^{-1}$ h^{-1} at 50 ºC; **12c**: 1.7 × 10^6 g mol(Ni)$^{-1}$ h^{-1} and **12d**: 2.1 × 10^6 g mol(Ni)$^{-1}$ h^{-1} at 50 ºC *vs.* 1.8 × 10^6 g mol(Ni)$^{-1}$ h^{-1} at 60 ºC; 40 atmospheres ethylene pressure], the catalyst stability also increased as well. The nature of the bridge (n = 0 or 1) did not have a clear effect on the polymerization activity which is borne out by comparison of the ^{i}Pr- and the 3,5-$(CF_3)_2C_6H_3$-substituted complexes. Conversely, the molecular weights were influenced by the reaction temperature leading to the expected decrease on raising the temperature. The M_n values of the polymers formed at 50 ºC for the binuclear complexes are significantly higher than those formed with the mononuclear analogues (*e.g.*, **12b**: 95 kg mol^{-1} *vs.* 24 kg mol^{-1} and for **12d**: 83 kg mol^{-1} *vs.* 12 kg mol^{-1}). In addition, the number of methyl branches observed in **12** is 4, as compared to 10 and 12 determined in the mononuclear cases. For polymers prepared at polymerization temperatures of 60 or 70 ºC, a small portion of ethyl branches (≤ 1/1000 Cs) was also observed. Moreover, the molecular weights correlate with the branching as *β*-H transfer is a key step for both the formation of branches as well as chain transfer; thus, with increased branching, molecular weights of the polyethylenes decrease.

A series of arene-bridged binuclear nickel complexes, **13**, **14** and **15**, are also shown in Fig. 5. The bimetallic complex **13b** displays higher activities (2.9 × 10^5 g mol(Ni)$^{-1}$ h^{-1}) for ethylene polymerization and affords polymer with higher molecular weight (M_w = 141 kg mol^{-1}) and broader molecular weight distribution (PDI = 6.1) than its mononuclear comparator and operates without any co-catalyst [63]. Although *tert*-butyl groups are generally considered to be bulkier than unsubstituted phenyl groups, phenyl is more electron-withdrawing than *tert*-butyl. Hence, it is reasonable that **13a** proved less active in ethylene polymerization when combined with *ca.* 2–3 equivalents of $Ni(COD)_2$ as phosphine scavenger. Methyl branching predominated with *ca*. 20 methyl branches per 1000 Cs. In addition, the distance between the two nickel centers is 7.654 Å.

Studies involving arene-bridged salicylaldimine-based binuclear neutral nickel complexes have been conducted by Huang's group [65]. In their research, the ten targeted complexes based around **14** (Fig. 5) were synthesized and used as catalysts in ethylene polymerization delivering high activities in the presence or absence of the phosphine scavenger $Ni(COD)_2$. Highly branched polyethylenes (46 − 127 branches/1000 Cs) with moderate molecular weights (M_η = 1.0 − 169 × 10 kg mol^{-1}) and narrow molecular weight distributions (2.3 − 2.4) were obtained using complexes **14a** – **14j** with or without $Ni(COD)_2$. Moreover, in comparison with the corresponding mononuclear analogue, the binuclear catalysts generally show higher thermal stability. Furthermore, complexes **14a**, **14c**, **14e** and **14f**, which possess small R^1 substituents, are capable of acting as single-component ethylene polymerization catalysts. In addition, the introduction of an electron-withdrawing group (**14i** and **14j**) to the ligand framework improves the catalytic activity significantly.

Agapie and co-workers reported that complete substitution of the central arene

blocks rotation around the aryl−aryl bond and allows for the isolation of atropisomers [54]. The solid-state structures of **15a** and **15b** (Fig. 5) revealed that the distance between the two metal centers is 7.1 Å in the *syn*-isomer and 11.1 Å in the *anti*-isomer, respectively. The structure of **15b** does not allow for cooperative reactivity because the two nickel centers are on opposite faces of the central arene. Ethylene polymerization screens were performed with **15a** and **15b** in toluene at 25 ºC with 7 atmospheres of ethylene pressure over 3 hours. These experiments generated polyethylene with methyl branches (4 − 20 branches per 1000 Cs). Without any additive, **15a** and **15b** gave good catalytic activities of 1.91×10^4 g mol(Ni)$^{-1}$ h^{-1} and 11.4×10^4 g mol(Ni)$^{-1}$ h^{-1}, respectively. However, in the presence of excess primary, secondary and tertiary amines, distinct inhibition effects were observed. For example, **15b** was inhibited by two orders of magnitude upon the addition of *N*,*N*-dimethylbutylamine, while **15a** by only one order of magnitude. This behavior is expected to have applications in the design of olefin polymerization catalysts with increased functional group tolerance and with the potential for copolymerization of polar olefins.

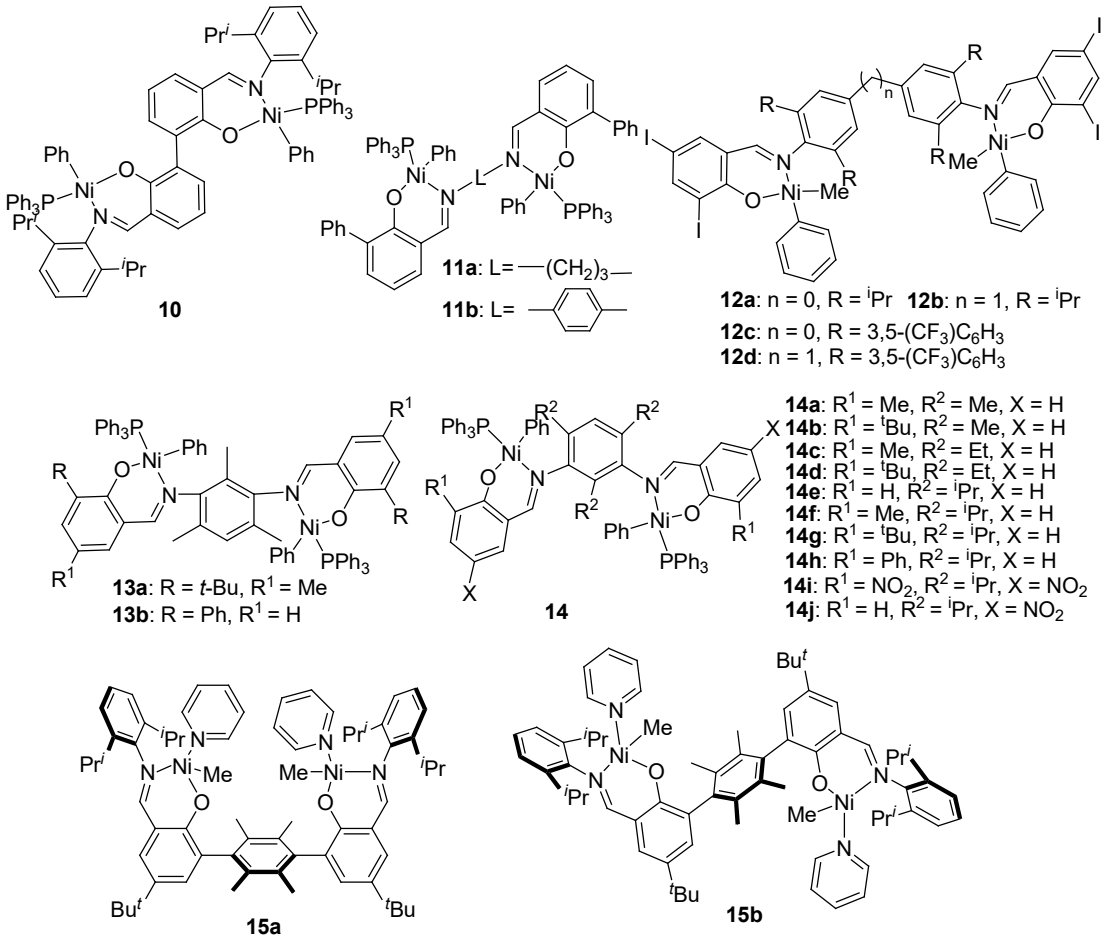

Fig. 5 Binuclear phenoxyimine-nickel complexes, **10** − **15**, with different types of linker

Other examples synthesized by Ma and co-workers have also been investigated as precatalysts in ethylene polymerization (Fig. 6). The rigid skeleton and bulky

tert-butyl groups together force the two nickel coordination planes closer, which caused a reduction in the Ni···Ni distance from 10.04 Å (**16c**) to 8.31 Å (**16b**) to 8.24 Å (**16a**), thereby inhibiting the rate of chain transfer relative to propagation and leading to the formation of high molecular weight polymers [13]. In the presence of $B(C_6F_5)_3$, which served as a phosphine scavenger, precatalyst **16** were screened in ethylene polymerization affording high activities up to 1.40×10^5 g(PE) mol(Ni)$^{-1}$ h^{-1} (**16a**) and a polymer with an M_n value of 38.6 kg mol^{-1} under 6 atmospheres of ethylene pressure, which represents an almost three-fold increase on that observed by its mononuclear counterpart (4.65×10^5 g(PE) mol(Ni)$^{-1}$ h^{-1}) and a two-fold increase in molecular weight (M_n =18.0 kg mol^{-1}). Different catalysts based on different linkers presented the following trend in activity: **16a** > **16b** > **16c**. A plausible explanation is that chain migration processes and chain termination side-reactions are expected to be suppressed when two nickel centers approach one another and simultaneously block the axial sites of each other, thus resulting in higher catalytic activity along with higher molecular weight [54, 56].

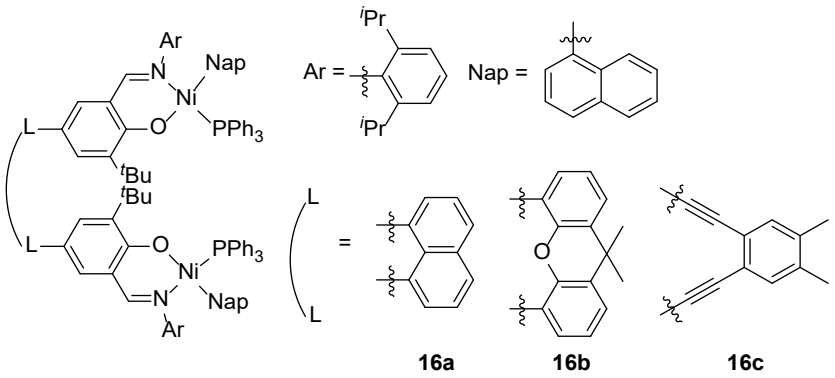

Fig. 6 Binuclear nickel complexes **16** bearing rigid linkers

Based on the structure of **C** (Scheme 2), Lee's group disclosed a series of unusual bimetallic nickel complexes incorporating macrocyclic tetraiminodiphenols, **17** (Fig. 7) [67]. The molecular structure of **17b** showed that the geometry around nickel is not unusual exhibiting a distorted square planar structure with a *trans*-relationship between the neutral phosphine ligand and the neutral imine ligand. The Ni···Ni separation distance is 8.869 Å, which is slightly longer than the O···O separation (7.255 Å). The activities of **17a** to **17c** are fairly good [$3.60 – 6.20 \times 10^5$ g(PE) mol(Ni)$^{-1}$h^{-1}], with **17a** showing the highest. When the polymerization temperature was raised to 40 ºC, the activities are reduced by about a half. Polymers obtained by the macrocyclic complexes contain branches (32 – 55 branches/1000 Cs). The M_w value of the polymers obtained by **17b** is significantly higher (37 – 38 kg mol^{-1}) than those seen for **17a** and **17c** (6.70 – 8.70 kg mol^{-1}) and exhibits rather broad molecular weight distributions (PDI: 5 – 10).

The molecular structure of **18** (Fig. 7) indicates that the two nickel centers are separated by a distance of 4.73 Å, which is shorter than that seen in the previously reported dinuclear salicylaldimine-nickel complexes (5.80 – 8.9 Å) [13, 54, 60, 63,

67]. **18** catalyzed the polymerization of ethylene in the presence of the phosphine scavenger [Ni(COD)$_2$]. **18** and its mononuclear counterpart differ significantly in the catalytic activity, which are 10.5 × 10^6 g(PE) mol(Ni)$^{-1}$ h^{-1} and 1.85 × 10^6 g(PE) mol(Ni)$^{-1}$ h^{-1}, respectively. The polyethylene produced using **18** displays a methyl-branched structure (59/1000 Cs) and a higher molecular weight (M_w = 12 kg mol^{-1}) than the polymerization catalyzed by the mononuclear analogue which yields a methyl- and ethyl-branched polymer (95/1000 Cs) with M_w = 1.7 kg mol^{-1}.

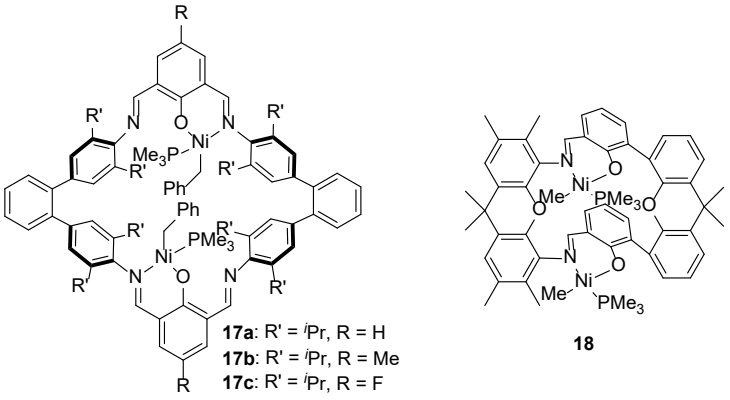

Fig. 7 Macrocyclic bimetallic nickel complexes **17** and **18**.

3.1.2 Cationic bimetallic α-diimine-nickel catalysts

A wide range of studies have been involved with developing bimetallic catalysts that incorporate two diimine pockets within the ligand manifold. To realize the synthesis, well-defined di-aniline units act as building blocks in the condensation protocol to form the linked diimines. This approach represents a straightforward means to generate a wide variety of binucleating ligands for olefin polymerization catalysts; indeed, such a synthetic strategy was first introduced in 1970 [72].

The binuclear nickel precatalysts (**19** – **22**) incorporating binucleating α-diimine ligands (Fig. 8) were readily prepared through condensation reactions from the xanthene-bridged di-anilines by Chen's group. Complexes **19** showed good thermal stability and high catalytic activity as well as producing high molecular weight polymer with narrow PDI and very low levels of branching [73]. Upon activation with MAO, the catalyst stability, the catalytic activity and the polyethylene molecular weight fell in the order: **19d** > **19c** ≈ **19b** > **19a**. The activity of **19d** can reach up to 5.0 × 10^6 g(PE) mol(Ni)$^{-1}$ h^{-1}, generating polyethylene with an M_n of 239 kg mol^{-1} when the polymerization was conducted at 20 ºC. In comparison with binuclear **19d**, the mononuclear counterparts showed lower activity (4.6 × 10^6 g(PE) mol(Ni)$^{-1}$h^{-1}) as well as lower molecular weight (M_n = 1.49 × 10^2 kg mol^{-1}). Moreover, at elevated temperature, the activity and molecular weight of the binuclear complexes was twice as high as that of the mononuclear ones. Notably, **20** maintained high activity even at 80 ºC. The molecular structure of **19d** revealed both nickel centers to adopt a distorted tetrahedral geometry resulting in a Ni···Ni distance of 7.757 Å, while the structure of **20** showed a shorter Ni···Ni distance of 3.618 Å, which may lead to a metal–metal

cooperativity effects during the polymerization. Most interestingly, the polyethylene generated by the dinuclear complexes possessed much lower degrees of branching (up to three times) than that generated by the corresponding mononuclear complexes. Metal–metal cooperativity effects were invoked to explain the slow *β*-H elimination process and the correspondingly slow chain-walking process, leading to this lower branching density. Meanwhile, the inhibition of rotation about the N-aryl moieties could also be responsible for the reduction in branching.

The related structures **21** and **22** (Fig. 8) reported by another Chen group [74] also exhibited, on activation with MAO, higher catalytic activities up to 2.2×10^6 g(PE) mol(Ni)$^{-1}$ h^{-1} for **21a**, higher molecular weights (M_n = 3.8 kg mol^{-1} for **21a**) and produced polyethylene with much lower branching (27/1000 Cs for **21b**) when compared with their mononuclear analogues. At 20 ºC, the polymerization activity decreased in the following order: **21a** > **22a** > **21b** > **22b**. Moreover, the degree of branching (27−88/1000 Cs) increased with polymerization temperature from 20 to 60 ºC. Interestingly, in the molecular structure of **22a**, two Br bridges were observed, leading to a short Ni···Ni distance (3.645 Å). However, upon activation during polymerization, the electrostatic repulsion between the two Ni centers may lead to a longer Ni···Ni distance.

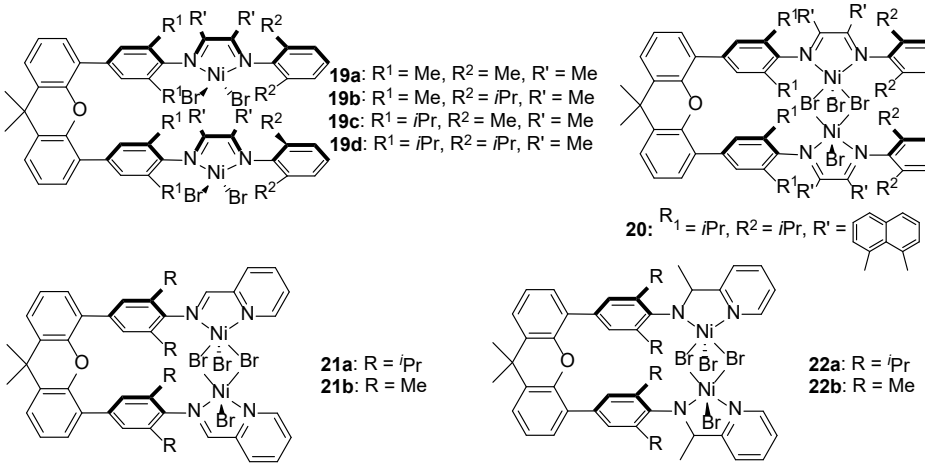

Fig. 8 Xanthene-bridged dinuclear nickel(II) complexes, **19** − **22**

Table 2 collects together selected information *(viz*., Ni···Ni distance, catalytic activity, molecular weight and branches) concerning various xanthene-bridged dinuclear nickel complexes. On inspection of the table, it appears that the shorter the Ni···Ni distance the higher the activities. In addition, dinuclear complexes gave higher molecular weights and less branching in comparison with their mononuclear counterparts. These results further highlight the potential applications of metal−metal cooperativity in controlling the ethylene polymerization process, especially the capability of slowing down *β*-hydride elimination and the corresponding chain-walking process.

Table 2 Properties displayed by 6-xanthene-bridged dinuclear nickel complexes

Precat.	D_{Ni-Ni} (Å)[a]	Activity [× 10^5 g(PE) mol(Ni)$^{-1}$ h^{-1}][b]	M_w (kg mol^{-1})[c]	Branches[d]
16b	8.31	0.998	29.4	29
18	4.73	105	12.0	59
19d	7.757	50.0	239	28
20	3.618	41.7	112	15
21a	[e]	22.0	3.80	40
22a	3.645	4.68	4.70	61

[a] Ni···Ni distance determined by single crystal X-ray diffraction.

[b] All catalytic activities are measured at their optimum conditions.

[c] Molecular weight determined by GPC, including M_n and M_w.

[d] Determined by ^{1}H NMR spectroscopy; expressed per 1000 carbons.

[e] Not determined.

Our group have also been involved in the design of novel binuclear nickel complexes, which include **23** [75], **24** [76], **25** [77], **26** [78] and **27** [79] (Fig. 9−11). In comparison with their mononuclear nickel counterparts, the methylene-bridged dinuclear nickel complexes **23** [75] and **24** [76] appear to act with two different active sites producing both polyethylenes and oligomers. The highest activity (3.34 × 10^5 g(PE) mol(Ni)$^{-1}$ h^{-1} of 4.84 × 10^4 g(oligomer) mol(Ni)$^{-1}$ h^{-1}) was obtained using **23b** (conditions: Al/Ni molar ratio of 1000 at 0 ºC within 30 minutes at 1 atmosphere ethylene). The M_w of the polymer was 8.20 kg mol^{-1} with a PDI of 3.66. Complex **23c**, containing isopropyl substituents, gave the highest catalytic activity (6.38 × 10^5 g(PE) mol(Ni)$^{-1}$ h^{-1} with 0.94 × 10^4 g(oligomer) mol(Ni)$^{-1}$ h^{-1}), while under the same reaction conditions, **23e** – **23h** displayed lower activities with the polyethylenes taking the form of wax-like materials. Though the bulkier group is recognized to increase the catalytic activity of late transition metal complexes, it is plausible that the conjugated system containing a phenyl substituent decreases the net charge of the active metal center leading to reduced activity. The ^{13}C NMR spectra of the polyethylene obtained using **23c** showed branched polyethylene containing vinyl unsaturated chain ends with mainly butyl branches; the extent of branching was determined as 5 branches per 1000 Cs.

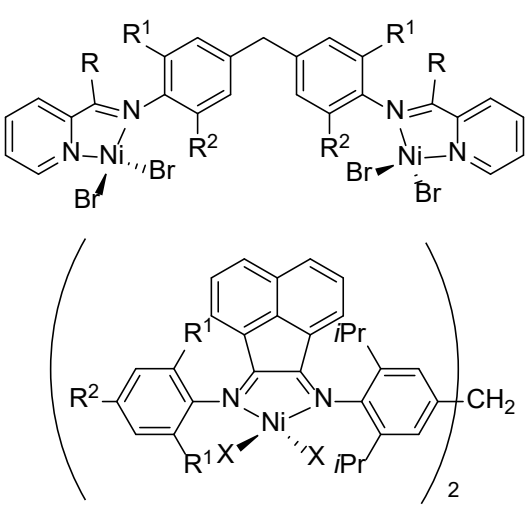

23a: R = H, R^1 = Me, R^2 = Me
23b: R = H, R^1 = Et, R^2 = Et
23c: R = H, R^1 = *i*Pr, R^2 = *i*Pr
23d: R = H, R^1 = *i*Pr, R^2 = Me
23e: R = Ph, R^1 = Me, R^2 = Me
23f: R = Ph, R^1 = Et, R^2 = Et
23g: R = Ph, R^1 = *i*Pr, R^2 = *i*Pr
23h: R = Ph, R^1 = *i*Pr, R^2 = Me

24a: R^1 = Me, R^2 = H, X = Br
24b: R^1 = Et, R^2 = H, X = Br
24c: R^1 = *i*Pr, R^2 = H, X = Br
24d: R^1 = Me, R^2 = Me, X = Br
24e: R^1 = Et, R^2 = Me, X = Br
24f: R^1 = Me, R^2 = Me, X = Cl

Fig. 9 Methylene-bridged dinickel(II) **23** and **24**

Complexes **24** represents another class of a methylene-bridged complex (Fig. 9) [76], which also gave higher activities when compared with its mononuclear analogs. The highest activity among these six complexes was observed with **24d**/DEAC of 7.86×10^6 g(PE) mol(Ni)$^{-1}$ h^{-1}, affording polymer with a M_w of 2.05×10^2 kg mol^{-1} and a PDI of 2.83 (conditions: Al:Ni molar ratio of 500 at 50 ºC within 30 minutes). Notably, these values are higher than their mononuclear counterparts (activity of 5.43×10^6 g(PE) mol(Ni)$^{-1}$ h^{-1}, M_w of 1.02×10^2 kg mol^{-1} and PDI of 1.95) under comparable conditions. The substituents present within the ligand manifold significantly affected the catalytic activities which fall in the order: **24d** (2,4,6-tri(Me)) > 2**4a** (2,6-di(Me)) > **24e** (2,6-di(Et)-4-Me) > **24b** (2,6-di(Et)) > **24c** (2,6-(*i*-Pr)). The chloride complex **24f** exhibited a slightly lower activity than its analogue **24d**. Based on the high temperature ^{13}C NMR data for **24d**, the main types of branches were methyl (41%) and ethyl (21%) as well as some longer chain branches, which is consistent with previous observations [80].

Rigid backbone-containing **25** revealed much longer lifetimes (Fig. 10) [77]. Activated by MAO (Al:Ni molar ratio of 500, 30 ºC, 30 minutes), the activity of **25a** can reach as high as 1.50×10^6 g(PE) mol(Ni)$^{-1}$h^{-1} and the polymer can display a narrow PDI of 2.2. On extending the reaction time to 60 minutes, the activity remained reasonably constant at 1.30×10^6 g(PE) mol(Ni)$^{-1}$h^{-1}, while the PDI broadened to 4.2. Precatalyst **25b** also showed high activity (1.26×10^6 g(PE) mol(Ni)$^{-1}$h^{-1}) but with a broader PDI (3.0) for the polymer.

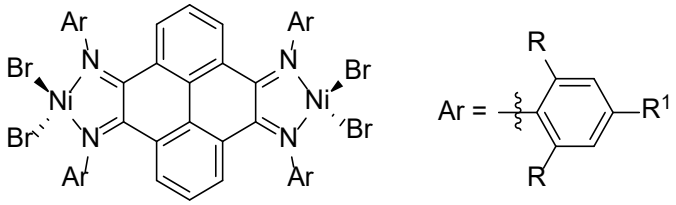

25a: R = Me, R^1 = H
25b: R = Me, R^1 = Me

Fig. 10 Rigid backbone-type binuclear nickel complex **25**

Similar bridged nickel complexes **26** [78] and **27** [79] (Fig. 11) also exhibited good activities towards ethylene polymerization. Upon treatment with MAO, the complex **26** activates the polymerization of ethylene to form polymer displaying M_w values in the range 12 − 66 kg mol^{-1} and PDI's from 1.4 to 5.4. Both **27**/Me_2AlCl and **27**/MAO systems gave superior activities (6.55 × 10^6 g(PE) mol(Ni)$^{-1}$ h^{-1}) but formed polymers with lower molecular weights (7.02 kg mol^{-1}).

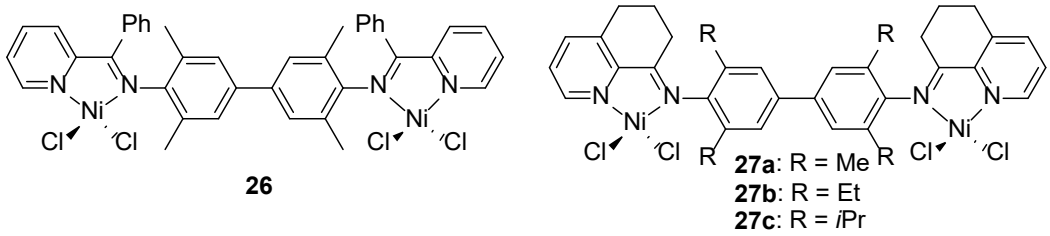

Fig. 11 Biphenyl-bridged binuclear nickel complexes **26** and **27**

Variation in the aryl linker group was also reported by Solan's group leading to a series of binuclear nickel complexes **28** and **29** (Fig. 12). Upon activation with excess MAO, **28a** and **28b** show some activity for alkene oligomerization forming low molecular-weight materials with methyl-branched products (158 *vs.* 50) [81]. Inspection of the intermetallic distance [5.223(4) Å] reveals that there is no direct Ni···Ni interaction between the two metal centers. Additionally, **29** [82] can afford mixtures of waxes and low molecular weight solid polyethylene with the activity falling in the order: **29b**/MAO > **29c**/MAO > **29a**/MAO > **29d**/MAO. The highest activity of 4.09 × 10^5 g mol(Ni)$^{-1}$h^{-1} (polymer and oligomer) was obtained using **29b**/MAO. All the systems produced low molecular weight polyethylene with broad molecular weight distributions.

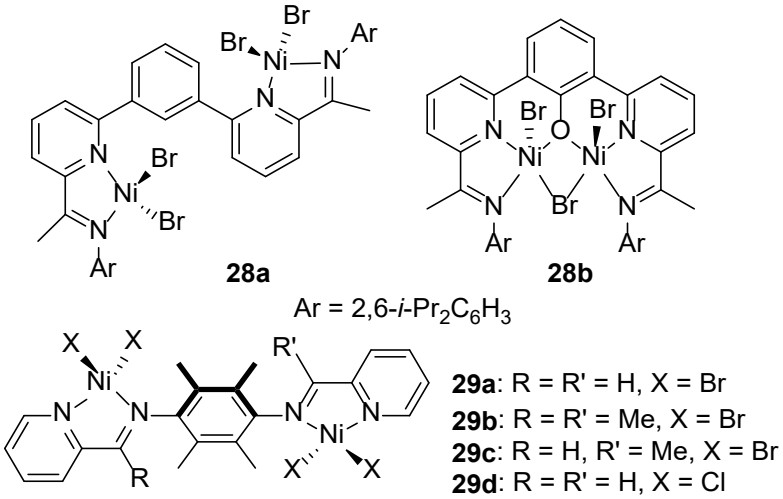

Fig. 12 Aryl-bridged binuclear nickel complexes **28** and **29**

3.2 Binuclear iron and cobalt precatalysts

As with the linked diimine-nickel precatalysts discussed in the previous section, there have been a number of investigations concerned with developing bimetallic iron or cobalt catalysts that incorporate two bis(imino)pyridine binding pockets within the same compartmental ligand [83-88]. Indeed, a wide variety of synthetic strategies have been employed including the use of di-aniline units as building blocks in the condensation protocol [89-93].

A potentially pentadentate nitrogen ligand and its complexes **30** were synthesized by Bianchini's group (Fig. 13) [83]. On activation with MAO, the iron and cobalt complexes generate effective catalysts for the oligomerization of ethylene to α-olefins with productivities and Schulz-Flory parameters depending on the type and number of the coordinated metals. The activity obtained by **30a** is 3.7×10^6 g mol(Fe)$^{-1}$ h^{-1}, whereas 3.4×10^6 g mol(Co)$^{-1}$ h^{-1} was observed by **30b**, which are both higher than their mononuclear analogues, especially in the Co case, **30b**, which is almost four-fold higher than the mononuclear one. The chain length of the oligomers showed a clear dependence on the nature of the metal center with C_4-C_{14} α-olefins produced with **30b** (K = 0.12), whereas iron-containing **30a** gave a broader oligomer distribution (K = 0.71) [Note: K = probability of propagation = $\text{rate}_{\text{propagation}}/(\text{rate}_{\text{propagation}} + \text{rate}_{\text{chain transfer}})$ = (moles of C_{n+2})/(moles of C_n)]. The ability of **30a** to produce higher molecular weight oligomers as compared to **30b** is typical of systems supported by 2,6-bis(imino)pyridine ligands in which one nitrogen atom bears an aryl substituent and the other a cyclohexyl [94].

The binuclear iron and cobalt complexes **31** and **32** have been used as catalyst precursors for the polymerization of ethylene to give high-density polyethylene (HDPE) on activation with MAO (Fig. 13) [84]. Under the conditions, 24 μmol catalysts, Al/M = 7200, 15 minutes, 25 ºC, **31a** showed the highest activity of up to 1.77×10^6 g mol(Fe)$^{-1}$ h^{-1}; complex **31b** gave 1.27×10^6 g mol(Co)$^{-1}$ h^{-1} and **31c** 1.47×10^6 g mol(Co)$^{-1}$ h^{-1}. Only the M_w value of the polymer obtained using **31b** was presented (439 kg mol^{-1}). The productivity of **32a** was almost identical to that of the mononuclear comparator, 4.73×10^6 g mol(Fe)$^{-1}$ h^{-1}, with an M_w of 413 kg mol^{-1}. It would appear that the coupling of two bis(imino)pyridine moieties *via* the pyridine C4 carbon atom does not noticeably influence the catalytic activity of the iron centers. Unlike **32a**, the dicobalt congener **32b** [5.37×10^6 g mol(Co)$^{-1}$h^{-1}] was significantly more active than the mono-cobalt bis(imino)pyridine catalyst [3.47×10^6 g mol(Co)$^{-1}$ h^{-1}].

Solan and co-workers found that on activation with MAO, **33** are considerably more active (**33b** > **33a**) with the most productive system, yielding uniquely linear α-olefins (Fig. 13) [87]. On the other hand, **34** showed only low activities for ethylene oligomerization (**34b**: 0.8×10^4 g mol(Co)$^{-1}$ h^{-1}) or was inactive (**34a**/MAO). Dicobalt and diiron systems bearing **31b** and **31a** are more selective and generate even-numbered linear α-olefins [> 98%; range: C_6–$C_{20} \geq C_{20}$ 0.28%, range: C_6–$C_{28} \geq C_{20}$ 29%] with the dicobalt system giving the higher of the activities (21×10^4 g

mol(Co)$^{-1}$ h^{-1} of **33b** *vs.* 1 × 10^4 g mol(Fe)$^{-1}$ h^{-1} **33a**). Both catalysts afford Schulz–Flory distributions for the α-olefins, with the *K* value being higher (0.78) for **33b** than for **33a** (0.58) consistent with a higher probability of chain propagation and the observed broader range of α-olefins.

Our group have also been committed to the development of new bimetallic skeletons, including **35** [85, 86] and **36** (Fig. 13) [88]. Based on the molecular structure of **35g** [86], an intermetallic distance of 4.979 Å reveals that there is no direct Co···Co interaction between the two metal centers. Activation with MMAO showed good catalytic activity for ethylene oligomerization and polymerization with a high selectivity for α-olefins; the detailed results are compiled in Table 3. The oligomerization and the polymerization activities as well as the *K* value varied in the order: **35a** (dimethyl) > **35b** (diethyl) > **35c** (diisopropyl). The introduction of a methyl group to the *para*-position (**35d**) led to lower activity and a higher percentage of polyethylene wax. Ethylene oligomerization/polymerization with the bimetallic cobalt analogues **35e**–**h**/MMAO were investigated under the same conditions (Al/Co molar ratio of 1000 and 30 ºC). It was observed that an increase in steric hindrance of the R^1 group led to decreased activity and lower *K* value. Very high activity was achieved at 60 ºC with **35e**: 7.38 × 10^6 g(oligomer) mol(Co)$^{-1}$ h^{-1} and 22.1 × 10^6 g(polymer) mol(Co)$^{-1}$ h^{-1}. The ^{13}C NMR spectra of the hydrocarbons generated using **35a** further demonstrated that linear α-olefins are the main species in the waxes.

The synthesis of **36** is not straightforward and involves a cyclization step in which 2,6-diacetylpyridine is condensed with 2-fluorobenzenamine to form a benzazepinyl ring (Scheme 5). This diketone was further reacted with two equivalents of the corresponding aniline and the resulting diimine complexed with the corresponding metal(II) halide (Scheme 5). All complexes **36a**–**j** (Fig. 13), when activated with MAO or MMAO, exhibited high activities of up to 4.0 × 10^7 g mol(Fe)$^{-1}$ h^{-1} for ethylene oligomerization and polymerization [88]. The iron precatalysts generally showed higher activities and produced broader distributions (PDI range: 1.47 – 8.9) of products (including oligomers and polyethylene) than their cobalt analogues (only oligomers). In addition, these bimetallic precatalysts exhibited higher (almost twice) activities in comparison to their monometallic analogues.

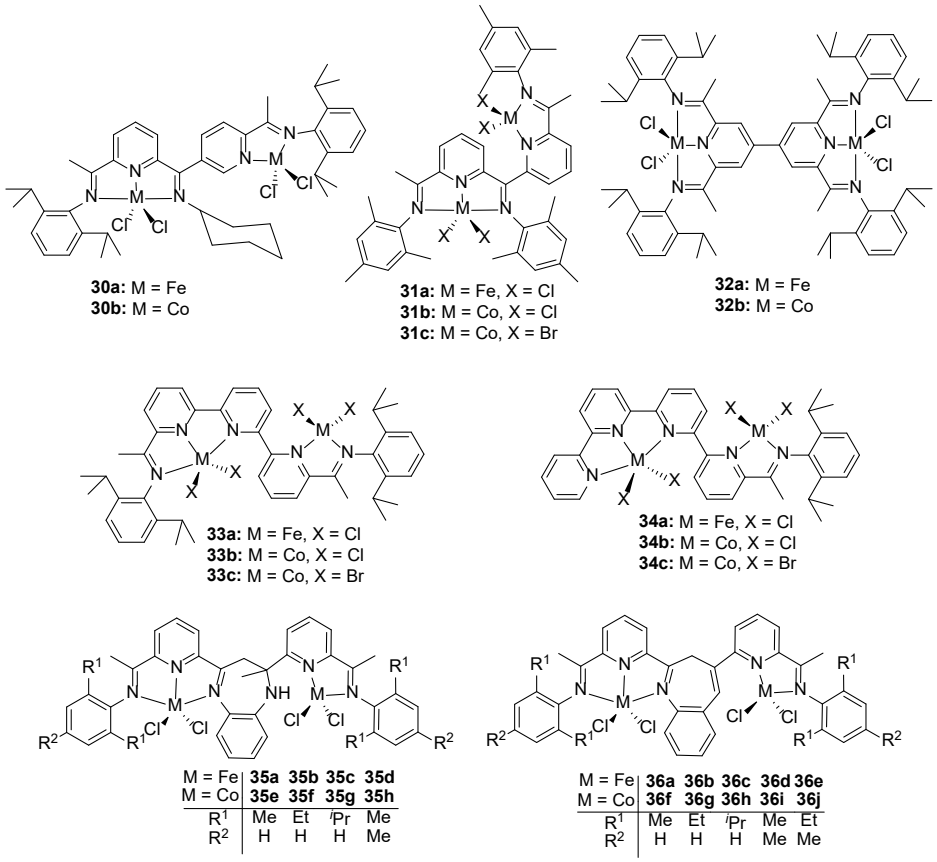

Fig. 13 Seven examples of bimetallic (Fe and Co) complexes, **30** – **36**

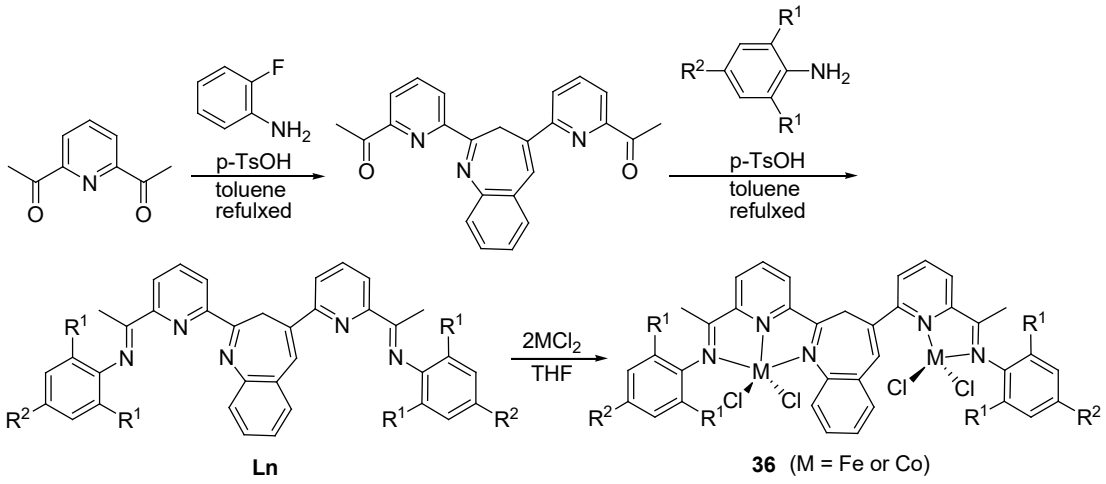

Scheme 5 Synthetic route to **36**

Table 3 Ethylene oligomerization and polymerization by complexes **35a**–**h**[a]

Precat.	Al/M	T/°C	Oligomer		Polymer
			Activity[b]	*K*[c]	Activity[b]
35a	1000	30	6.17	0.71	4.15

35b	1000	30	1.36	0.61	1.19
35c	1000	30	0.46	0.59	0.30
35d	1000	30	2.98	0.62	3.46
35e	1000	30	1.83	0.64	1.36
35f	1000	30	0.81	0.57	0.74
35g	1000	30	0.73	0.53	0.45
35h	1000	30	2.02	0.57	1.35
35e	1500	60	7.38	0.80	22.1

[a] General conditions: Precat.: 2.5 μmol; co-cat.: MMAO; reaction time: 30 min; ethylene pressure: 30 atm; solvent: toluene (100 mL).

[b] Activity for oligomers or polymers: $\times 10^6$ g mol(M)$^{-1}$ h^{-1}.

[c] The probability of propagation

As has been mentioned earlier, the application of novel diamine building blocks as a means of forming new imine-based ligand backbones for bimetallic complexes is as approach that is receiving growing attention (see **37** – **40**, Fig. 14) [89-93]. Methylene-bridged binuclear bis(imino)pyridine-iron(II) complexes **37a** show very poor activity for the polymerization of ethylene at 1 atmosphere of ethylene pressure, whereas, **37b** and **37c** exhibit much higher activity than the mononuclear iron counterparts in the presence of Al(*i*-Bu)$_3$; a finding that has been attributed to the reduced capacity of Al(*i*-Bu)$_3$ to undergo chain-transfer reactions [89]. The M_w values of the polyethylene produced by **37b** and **37c** were in the range 132 – 460 kg mol^{-1} and much higher than those produced by their mononuclear analogues. GPC results demonstrate that **37b** and **37c** yield polyethylene with a broad bimodal molecular weight distribution. Moreover, increasing the temperature and the Al/Fe molar ratio leads to a narrowing of the PDI of the polyethylene.

Exchange of the methylene-bridge for a biphenyl-bridge yields the diiron and dicobalt complexes **38** (Fig. 14), which have been the subject of an in-depth ethylene polymerization screen [90, 91]. All iron complexes **38a**–**k**, when activated by MAO or MMAO, exhibited high activities of up to 13.1 $\times 10^6$ g mol(Fe)$^{-1}$ h^{-1} (**38b**) [91]. On comparison with their mononuclear counterparts, these bimetallic complexes not only retain a high activity at elevated temperatures (up to 70 ºC, 11.1 $\times 10^6$ g mol(Fe)$^{-1}$ h^{-1}), but also exhibit increased lifetimes (6.70 $\times 10^6$ g mol(Fe)$^{-1}$ h^{-1}). 2,6-Diethyl-containing **38b** exhibited higher activities than the analogs **38a** and **38c**, which is consistent with previous observations for bis(imino)pyridine-iron pre-catalysts due to the favorable steric properties of the ethyl substituent compared to methyl and *i*-propyl [95]. Comparing **38d** – **38f**, derived from tetraethylbenzidine, with **38g** – **38i** from tetra(isopropyl)benzidine, the catalytic activities decreased with more sterically demanding R^3 substituents, indicating that the ethylene coordination and insertion became slower when bulky substituents surrounded the metal centers [96]. The highest M_w of the polymer of 283 kg mol^{-1} was achieved using **38g** and exhibited a bimodal distribution. Similarly, cobalt counterparts **38l**–**v**, upon activation

with either MAO or MMAO, gave extremely high activities of up to 7.7 × 10^6 g mol(Co)$^{-1}$ h^{-1} (**38r**) for ethylene polymerization, which indeed represents one of the most active cobalt-based catalytic systems reported to date [90]. However, the M_w's obtained were significantly smaller than their iron analogues, ranging from 1.1 – 120.6 kg mol^{-1}, while the resultant polyethylenes were generally highly linear. Furthermore, under optimized conditions, the polyethylene generated exhibited a narrow PDI (*ca.* 2), indicating single-site character for the active species.

Recently, we have disclosed our results on using methylene-bridged bimetallic bis(imino)pyridine-cobaltous chlorides **39** as precatalysts in ethylene polymerization (Fig. 14) [92]. The molecular structure of **39a** shows the two metal centers to be separated by a distance of 13.339 Å with each cobalt center displaying a distorted trigonal bipyramidal geometry. On activation with either MAO or MMAO, **39a** – **39d** exhibited high activities for ethylene polymerization (up to 14.6 × 10^6 g(PE) mol^{-1}(Co) h^{-1} at 50 ºC with Al/Co molar ratio of 2250 using **39a** with their relative values influenced by the steric properties of the N-aryl groups: **39a** > **39c** > **39d** > **39b**. Highly linear polyethylenes incorporating high degrees of vinyl end-groups are a feature of all the materials produced with the molecular weights of the MAO-promoted systems (M_w range = 2 – 8 kg mol^{-1}) generally higher than seen with MMAO (M_w range = 1 – 3 kg mol^{-1}), while the distributions using MMAO are narrower (PDI < 2.0). Evidence is presented that the MAO-promoted polymerizations have a preference for a termination mechanism involving *β*-H transfer to metal or to the monomer [95], while transfer to aluminum is competitive in the MMAO-promoted case.

For purposes of comparison, four of the most productive precatalysts (**37** – **39**) have been selected to compare their stability, catalytic activity, molecular weight, PDI and T_m values (Table 4). On examination of the tabulated data, **38g** showed superior thermal stability, higher activity, when compared with **37b**, though the M_w was significantly lower (*ca*. 70%). It is plausible to hypothesize that the bulkier substituents on the *ortho*-positions of the N-aryl group retard the monomer insertion step, leading ultimately to lower activity. **38r** and **39a** showed similar activity, while **39a** gave polyethylene waxes with vinyl end-groups, which is consistent with the lowest molecular weight and T_m value.

Table 4 Results of ethylene polymerization studies using complexes **37** – **39**

Precat.	Co-cat.	Al/M	T/ºC	t/min	Activity[a]	M_W[b]	M_w/M_n[b]	T_m[c]/ºC
37b	$AlEt_3$	2000	0	20	6.24	217	28.7	131.1
38b	MAO	1500	60	30	13.1	66.1	9.5	132.5
38r	MAO	1000	50	30	7.7	10.8	2.3	130.0
39a	MAO	2250	50	30	8.89	2.3	2.2	121.5

[a] Activity: × 10^6 g(PE)·mol^{-1}(M)·h^{-1}.

[b] M_w in kg mol^{-1}. M_w and M_w/M_n determined by GPC.

[c] Determined by DSC.

The macrocyclic iron and cobalt complexes **40** based on a double-decker structure were synthesized by linking two bis(imino)pyridine groups (Fig. 14) [93]. The molecular structure of **40b** revealed that the two bis(imino)pyridine-cobalt moieties stack in an antiparallel manner with a Co···Co distance of 7.74 Å. **40a** catalyzes the polymerization of ethylene at 80 − 120 ºC (5 atmospheres of ethylene) to produce polymers displaying relatively narrow molecular weight distributions (PDI = 1.75 − 2.77); the highest activity was 4.88 × 10^6 g(PE) mol^{-1}(Co) h^{-1} at 100 ºC. Surprisingly, polymers produced at room temperature under 1 atmosphere of ethylene by **40a** and **40b** gave much higher molecular weight (M_n up to 15-fold increase) than their corresponding mononuclear complexes under comparable conditions. Cooperative interactions between the growing polymer and the second metal center have been suggested as a means of retarding the undesirable deactivation of the catalyst and/or chain transfer.

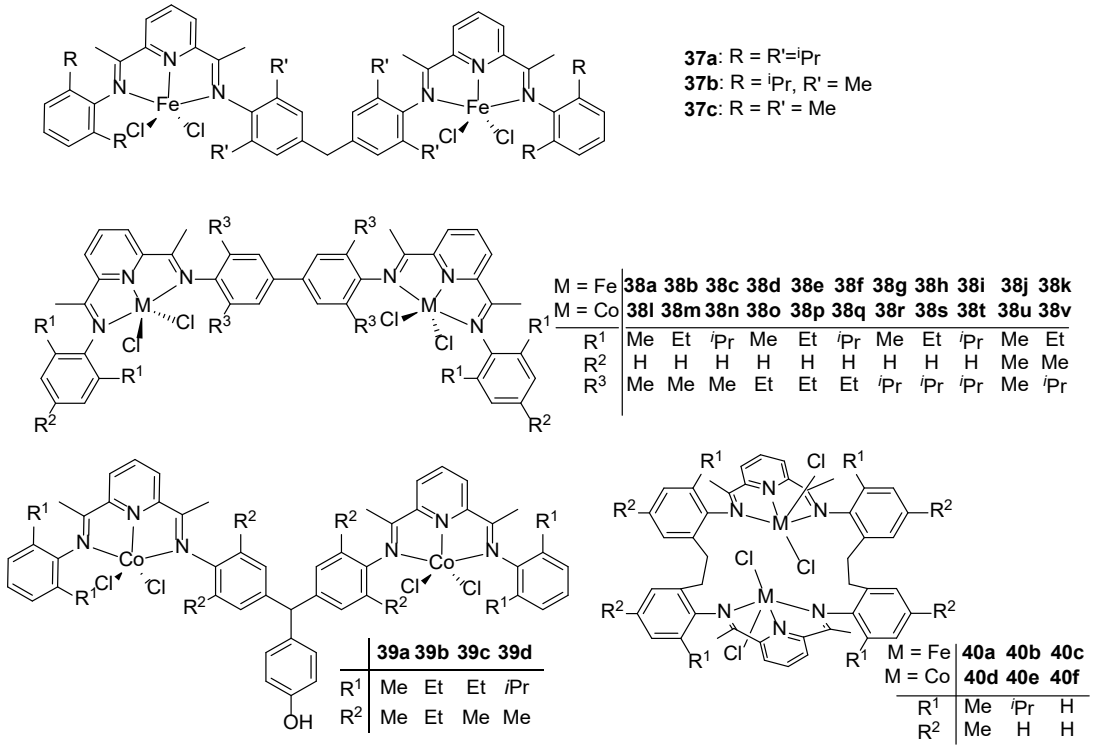

Fig. 14 Variation in the linker used to bridge the iron and cobalt complexes

4. Heterobimetallic catalysts

With a view to incorporating two different polymerization-active metal centers with distinct performance characteristics on the same ligand framework, a number of reports on the subject have appeared in recent years. While more synthetically challenging than their homobimetallic counterparts, the potential of these mixed-metal catalysts to deliver new or improved polymer properties has help drive early reports in

this area.

Marks and coworkers designed the linked mixed-metal CGC TiZr complex **41**, using a protodeamination and Al_2Me_6 alkylation methodology (Scheme 6), which in the presence of a diborate anion, polymerized ethylene to form polymers with long chain branches (number of carbons ≥ 6); this branching feature was ascribed to competing macromonomer re-enchainment [34, 97]. For example, one metal center (Zr) can produce α-olefins which are subsequently incorporated at the second metal center (Ti) to give high molecular weight polyethylene. At 65 ºC and within one minute, the highest activity of 2.8×10^6 g(PE) mol^{-1}(M) h^{-1} was achieved with the polymer possessing a M_w of 782 kg mol^{-1}. In comparison, a 1:1 mixture of the mononuclear Me_2Si-(^{t}BuN)(η^5-3-ethylindenyl)$ZrMe_2$ and Me_2Si(^{t}BuN)-(η^5-3-ethylindenyl)$TiMe_2$ in the presence of $Ph_3C^+B(C_6F_5)^-_4$ generates polymeric products with a bimodal distribution and negligible branching. In general, **41** produces monomodal polyethylene with significantly higher M_w's than simple mononuclear catalyst mixtures but with only ~2 branches (≥ C_6) per 1000 Cs, reflecting the limited activity and chain-transfer characteristics of these catalysts.

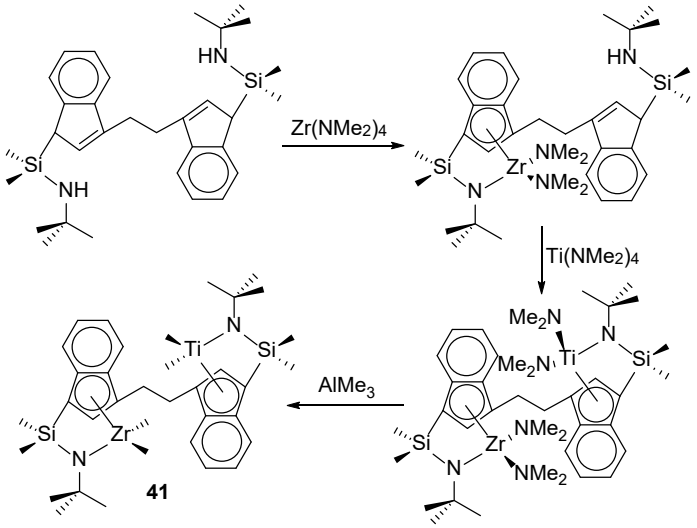

Scheme 6 Synthetic route to heterobimetallic **41**

A series of group 4−group 6 heterobimetallic TiCr olefin polymerization precatalysts **42**, has also been reported by Marks (Fig. 15) [35, 36]. On activation with MAO, complexes Ti-C_0-Cr^{SNS} (**42a**), Ti-C_2-Cr^{SNS} (**42b**), and Ti-C_6-Cr^{SNS} (**42c**) afford linear low density polyethylenes (LLDPEs) with exclusively *n*-butyl branches (6.8 − 25.8 branches/1000 Cs). On the other hand, **41** and its analogues produce polyethylenes with heterogeneous branching (C_2, C_4, and $C_{\geq 6}$) or negligible branching, respectively. Under identical conditions (Al/M = 500, 50 mL toluene, 5 minutes, 80 ºC, 8 atmospheres ethylene), **42a** produces polyethylenes with the highest activity [9.84×10^5 g(PE) mol^{-1}(M) h^{-1}], with the polymer displaying an M_w of 593 kg mol^{-1} and a branching content of 25.8/1000 Cs. These values compare to 2.21×10^5 g(PE) mol^{-1}(M) h^{-1}, 461 kg mol^{-1} and 8.2/1000 Cs for **42b** and 1.61×10^5 g(PE) mol^{-1}(M) h^{-1},

319 kg mol^{-1} and 6.8/1000 Cs for **42c**. Based on DFT calculations, the Ti···Cr distance was optimized as 6.0 Å for **42a**, 8.1 Å for **42b**, and 13.2 Å for **42c**, which proved consistent with the single crystal X-ray results. In addition, C_6 fragments are produced by the known sequence of reductive ethylene coupling and metallacyclopentene expansion to form a metallacycloheptane (**E** in Scheme 7) followed by reductive elimination, yielding 1-hexene.

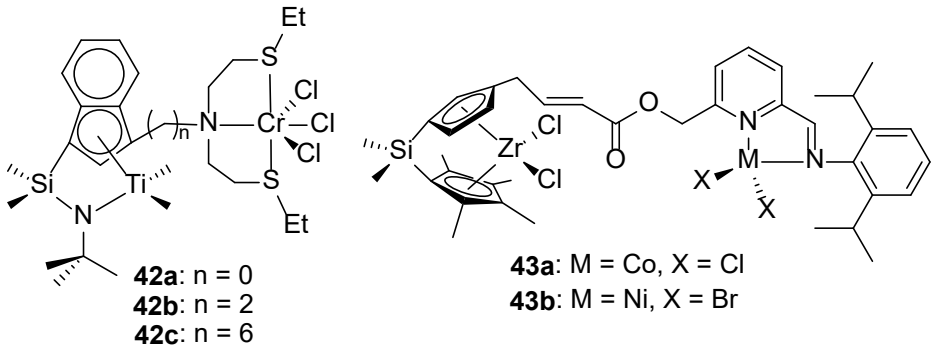

Fig. 15 Mixed-metal bimetallic transition metal complexes, **42** and **43**

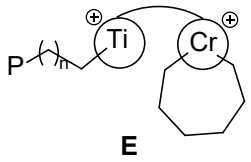

Scheme 7 Metallacycloheptane formation at chromium in **E**

Ethylene polymerization mediated by transition metal complexes containing both group 4 and 9/10 centers have been used to generate polymers with different branched structures and properties depending on the type of late transition-metal used (*e.g.*, **43** in Fig. 15) [98]. In terms of synthesis **43** were prepared by the selective cross-metathesis shown in Scheme 8. ZrCo **43a** and ZrNi **43b** exhibited similar activities (1.88 × 10^5 g(PE) mol^{-1}(M) h^{-1} *vs.* 2.17 × 10^5 g(PE) mol^{-1}(M) h^{-1}), but the polymer obtained using **43b** showed the presence of methyl as well as longer chain branches while **43a** only gave ethyl branches (Fig. 15). It would seem likely that the dinuclear ZrNi complex **43b** enables the efficient enchainment of a branched oligomer formed at the Ni center to the polymer chain grown at the Zr center. The molecular structure of **43a** was also reported revealing the Zr and Co atoms to be separated by a distance of *ca.* 9.1 Å.

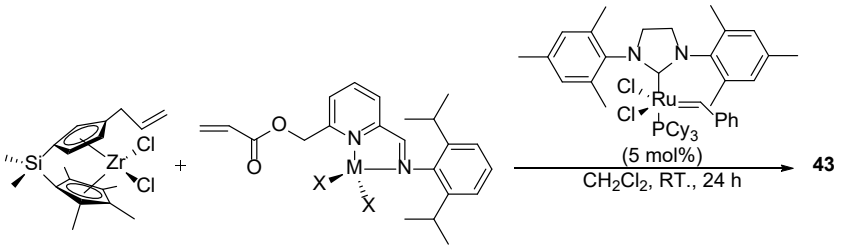

Scheme 8 Synthetic route to **43**

Nagashima and co-workers successfully used an azanickellacyclopentene to complex metal(II) bromides to form bimetallic MNi (M = Fe, Co) precatalysts **44** (Fig. 16). The azanickellacyclopentene itself can be synthesized by treatment of $Ni(COD)_2$ with CN(2,6-xylyl) and MeI in 89% yield (Scheme 9) [99]. FeNi **44b** exhibits high activity for ethylene polymerization [1.62×10^6 g(PE) mol^{-1}(Ni) h^{-1}] and generates polymer displaying a bimodal GPC profile (PDI: 3.4) which lends some support for the involvement of the second metal as an active center for the polymerization. The monomodal GPC profile (PDI: 2.9) as well as low activity [0.70×10^6 g(PE) mol^{-1}(Ni) h^{-1}] using CoNi **44a** show this is unlikely in this case. One explanation proposed for the second metal effect is the involvement of a structural change of the azanickellacyclopentene by incorporation of the second metal.

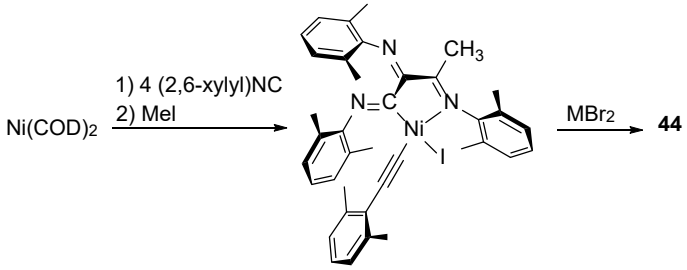

Scheme 9 Synthetic route to **44**

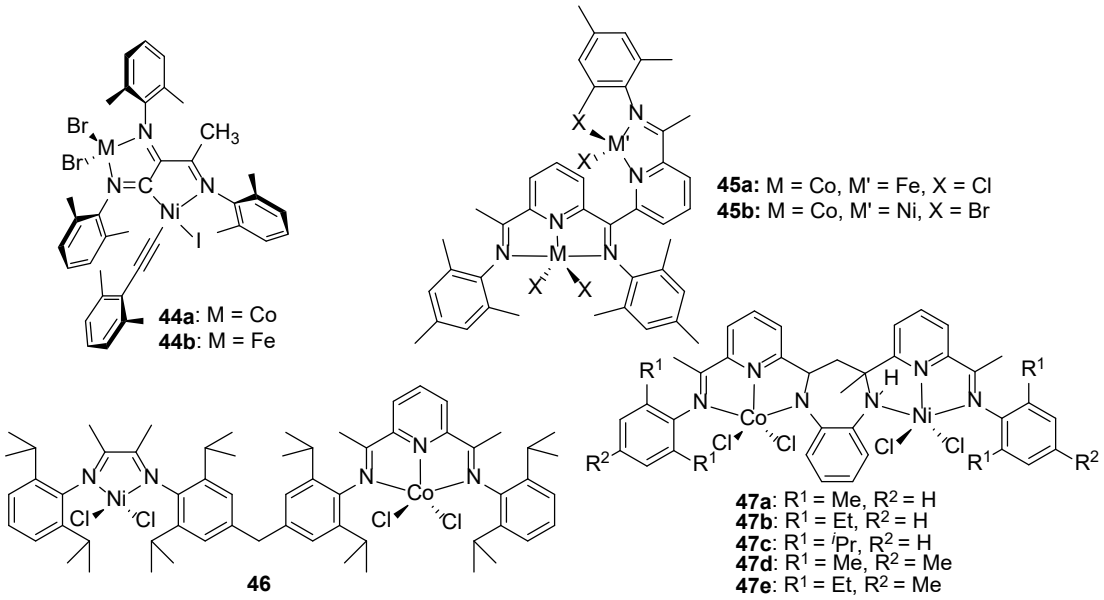

Fig. 16 Heterobimetallic late transition metal complexes, **44** – **47**

In addition to the homobimetallic complexes **31** and **32** discussed earlier (Fig. 13), Bianchini and co-workers also reported the catalytic performance of the heterobimetallic CoM (M = Fe, Ni) complexes **45** (Fig. 16) [84]. By using the same conditions (24 μmol catalysts, Al/M = 7200, 15 minutes, 25 ºC), **45a** and **45b** gave similar activities towards ethylene polymerization, 0.95×10^6 g(PE) mol^{-1}(M) h^{-1} and 0.88×10^6 g(PE) mol^{-1}(M) h^{-1}, respectively, which are 50% lower than seen for **31a**

(1.77×10^6 g mol(Fe)$^{-1}$ h^{-1}).

The NiCo complex **46** was synthesized by Fan's group and was compared with its monometallic cobalt and nickel counterparts in ethylene polymerization (Fig. 16) [100]. On activation with MMAO, **46** displayed only low polymerization activity of [1.64×10^6 g(PE) mol^{-1}(M) h^{-1}] when compared to its mononuclear counterparts [*i.e.*, 3.40×10^6 g(PE) mol^{-1}(Co) h^{-1} and 1.95×10^6 g(PE) mol^{-1}(Ni) h^{-1}]. It also showed higher molecular weight (M_w = 48.4 kg mol^{-1}) and a broader PDI (5.73) characteristic of bimodal character. The branches per 1000 Cs of polyethylene produced by **46** is 57.7 which compares with 84.5 for the mono-nickel comparator. These results reveal that the productivity of the nickel center of the binuclear complex is predominantly suppressed due to selective activation of the metallic center in the heterobinuclear complex.

Using the same binucleating ligand frame as used for homobimetallic **35** (Fig. 13), NiCo **47** was synthesized by our group (Fig. 16) [101]. On activation with MAO, the catalytic behavior of **47** was found to follow a Poisson distribution. Inspection of the intermetallic Ni···Co distance of 4.965 Å in **47c** reveals no direct interaction and is comparable with the Co···Co length of 4.979 Å in **35b** [86] but slightly longer than the Ni···Ni distance of 4.717 Å in the dinickel derivative [85]. Generally, all the mononuclear cobalt comparators and NiCo **47** showed good activities towards ethylene reactivity (oligomerization and polymerization), though the mononuclear cobalt complexes were at the top end of the activity scale [8.9×10^6 g(oligomers) mol^{-1}(Co) h^{-1} *vs.* 2.8×10^6 g(oligomers) mol^{-1}(M) h^{-1} (**47**)]. This lowering in activity observed in these mixed-metal complexes has been described as the '*frustratingly synergic effect*' in ethylene oligomerization. Moreover, when compared with its Co_2 counterparts **35e**–**h**, **47d** displayed superior catalytic activity, while **47a** to **47c** exhibited one tenth the activity displayed by **35h** (Table 5).

Table 5 Ethylene oligo-/polymerization using **35e**–**h**/MMAO or **47**/MMAO[a]

Precat.	Al/M	Oligomer		Polymer	
		Activity[b]	K[c]	Activity[b]	PE (wt%)[d]
35e	1000	1.83	0.64	1.36	42.6
35f	1000	0.81	0.57	0.74	47.7
35g	1000	0.73	0.53	0.45	38.1
35h	1000	2.02	0.57	1.35	40.1
47a	1500	0.2	[e]	0.12	38
47b	1500	0.2	[e]	0.12	38
47c	1500	0.2	[e]	0.19	49
47d	1500	2.8	[e]	0.36	11

[a] General conditions: 2.0 μmol of complex; ethylene pressure: 10 atm; polymerization time: 30 min; reaction temperature: 30 ºC; 100 mL of toluene as solvent.

[b] Activity: × 10^6 g(oligomers) mol^{-1}(M) h^{-1}.

[c] The probability of propagation

[d] The percentage of polyethylene wax.

[e] Not calculated.

5. Conclusions and outlook

From the work presented in this review, it is clear that suitably designed binuclear ethylene polymerization catalysts can afford different polymerization activities as well as unique polyolefin microstructures, when compared with their mononuclear analogues. One of the distinctive features displayed by these binuclear catalysts is that, in most cases, they exhibit greater catalytic activity per metal center than their mononuclear counterparts. Additionally, they can produce highly branched polyethylenes as well as enhance the observed molecular weight of the material. Of particular note is the proposal of binuclear agostic interactions and their role in influencing the β-H elimination/re-insertion kinetics of a chain-walking process. While good spatial proximity of the two metal centers appears an important factor on potential cooperativity, it is likely that the type of linker and its ability to balance electrons between active sites also plays a role.

Notwithstanding the potential of the above, the main drawbacks of these compartmentalized bimetallic complexes relates to the non-straightforward and sometimes costly synthetic routes to the ligands. Furthermore, difficulties with characterization of the complexes and in particular in growing single crystals to confirm the structural identity, creates further hurdles. Nevertheless, developments in dianiline synthesis has provided a growing selection of building blocks that make imine-based binucleating ligands much more accessible. Overall, it is our view that there remains many possibilities in this area relating to ligand design/synthesis, types of metal-metal combinations and the understanding of reaction mechanism which in-turn may open the door to new or improved polymeric materials.

Acknowledgements

This work is supported by the National Natural Science Foundation of China (U1362204 and 21374123). G.A.S. thanks the Chinese Academy of Sciences for a Visiting Scientist Fellowship.

GLOSSARY

CGC	Constrained geometry catalyst
COD	1,5-Cyclooctadiene
DEAC	Diethylaluminum chloride, Et_2AlCl

DSC	Differential Scanning Calorimetry
DMAC	Dimethylaluminum chloride, Me_2AlCl
DFT	Density functional theory
EASC	Ethyl aluminum sesquichloride, $Et_3Al_2Cl_3$
ETA	Ethyl trichloroacetate
Et_3Al	Triethylaluminum
FI	Phenoxyimine
g PE mol^{-1} (M) h^{-1}	Grams of polyethylene per mole of metal catalyst per hour
GPC	Gel Permeation Chromatography
K value	The probability of propagation
HDPE	High density polyethylene
LLDPE	Linear low density polyethylene
MAO	Methylaluminoxane
MMAO	Modified methylaluminoxane
M_n	Number-average molecular weight
M_w	Weight-average molecular weight
M_η	Viscosity-average molecular weight
NMR	Nuclear magnetic resonance
PDI	Polydispersity index
py	Pyridine, C_5H_5N
PE	Polyethylene
THF	Tetrahydrofuran
T_m	Melting temperature
tmeda	Tetramethylethylenediamine

References

[1] J.P. McInnis, M. Delferro, T.J. Marks, Acc. Chem. Res., 47 (2014) 2545-2557.

[2] B.L. Small, Acc. Chem. Res., 48 (2015) 2599-2611.

[3] V.C. Gibson, C. Redshaw, G.A. Solan, Chem. Rev., 107 (2007) 1745-1776.

[4] V.C. Gibson, S.K. Spitzmesser, Chem. Rev., 103 (2003) 283-316.

[5] C. Redshaw, Y. Tang, Chem. Soc. Rev., 41 (2012) 4484-4510.

[6] L. Zhong, G. Li, G. Liang, H. Gao, Q. Wu, Macromolecules, 50 (2017) 2675-2682.

[7] Z. Wang, G.A. Solan, Q. Mahmood, Q. Liu, Y. Ma, X. Hao, W.-H. Sun, Organometallics, 37 (2018) 380-389.

[8] J.L. Rhinehart, N.E. Mitchell, B.K. Long, ACS Catal., 4 (2014) 2501-2504.

[9] D.H. Camacho, Z. Guan, Chem. Commun., 46 (2010) 7879-7893.

[10] C. Bianchini, G. Giambastiani, I.G. Rios, G. Mantovani, A. Meli, A.M. Segarra, Coord. Chem. Rev., 250 (2006) 1391-1418.

[11] Z. Wang, Q. Liu, G.A. Solan, W.-H. Sun, Coord. Chem. Rev., 350 (2017) 68-83.
[12] Z. Wang, G.A. Solan, W. Zhang, W.-H. Sun, Coord. Chem. Rev., 363 (2018) 92-108.
[13] Z. Chen, E. Yao, J. Wang, X. Gong, Y. Ma, Macromolecules, 49 (2016) 8848-8854.
[14] L.K. Johnson, C.M. Killian, M. Brookhart, J. Am. Chem. Soc., 117 (1995) 6414-6415.
[15] M. Delferro, T.J. Marks, Chem. Rev., 111 (2011) 2450-2485.
[16] H. Makio, H. Terao, A. Iwashita, T. Fujita, Chem. Rev., 111 (2011) 2363-2449.
[17] R.M. Haak, S.J. Wezenberg, A.W. Kleij, Chem. Commun., 46 (2010) 2713-2723.
[18] H. Li, T.J. Marks, Proc. Natl. Acad. Sci. U.S.A., 103 (2006) 15295-15302.
[19] A. Motta, I.L. Fragalà, T.J. Marks, J. Am. Chem. Soc., 131 (2009) 3974-3984.
[20] M. Mitani, J. Saito, S.i. Ishii, Y. Nakayama, H. Makio, N. Matsukawa, S. Matsui, J.i. Mohri, R. Furuyama, H. Terao, H. Bando, H. Tanaka, T. Fujita, Chem. Record, 4 (2004) 137-158.
[21] H. Makio, T. Fujita, Acc. Chem. Res., 42 (2009) 1532-1544.
[22] A.L. McKnight, R.M. Waymouth, Chem. Rev., 98 (1998) 2587-2598.
[23] J. Klosin, P.P. Fontaine, R. Figueroa, Acc. Chem. Res., 48 (2015) 2004-2016.
[24] (a) V. C. Gibson, G. A. Solan, in Catalysis without Precious Metals (Ed. M. Bullock), Wiley-VCH, Weinheim, (2010) 111-141; (b) V. C. Gibson, G. A. Solan, Top. Organomet. Chem. 26 (2009) 107-158.
[25] Z. Flisak, W.-H. Sun, ACS Catal., 5 (2015) 4713-4724.
[26] C. Bianchini, G. Giambastiani, L. Luconi, A. Meli, Coord. Chem. Rev., 254 (2010) 431-455.
[27] M.R. Salata, T.J. Marks, J. Am. Chem. Soc., 130 (2008) 12-13.
[28] M.R. Salata, T.J. Marks, Macromolecules, 42 (2009) 1920-1933.
[29] H. Li, L. Li, D.J. Schwartz, M.V. Metz, T.J. Marks, L. Liable-Sands, A.L. Rheingold, J. Am. Chem. Soc., 127 (2005) 14756-14768.
[30] H. Li, L. Li, T.J. Marks, L. Liable-Sands, A.L. Rheingold, J. Am. Chem. Soc., 125 (2003) 10788-10789.
[31] N. Guo, L. Li, T.J. Marks, J. Am. Chem. Soc., 126 (2004) 6542-6543.
[32] H. Li, L. Li, T.J. Marks, Angew. Chem. Int. Ed., 43 (2004) 4937-4940.
[33] L. Li, M.V. Metz, H. Li, M.-C. Chen, T.J. Marks, L. Liable-Sands, A.L. Rheingold, J. Am. Chem. Soc., 124 (2002) 12725-12741.
[34] J. Wang, H. Li, N. Guo, L. Li, C.L. Stern, T.J. Marks, Organometallics, 23 (2004) 5112-5114.
[35] S. Liu, A. Motta, A.R. Mouat, M. Delferro, T.J. Marks, J. Am. Chem. Soc., 136 (2014) 10460-10469.
[36] S. Liu, A. Motta, M. Delferro, T.J. Marks, J. Am. Chem. Soc., 135 (2013) 8830-8833.
[37] S. Han, E. Yao, W. Qin, S. Zhang, Y. Ma, Macromolecules, 45 (2012) 4054-4059.
[38] C. Redshaw, Dalton Trans., 39 (2010) 5595-5604.
[39] K. Nomura, S. Zhang, Chem. Rev., 111 (2011) 2342-2362.
[40] J. Wu, Y. Li, Coord. Chem. Rev., 255 (2011) 2303-2314.
[41] L. Clowes, M. Walton, C. Redshaw, Y. Chao, A. Walton, P. Elo, V. Sumerin, D.L. Hughes, Catal. Sci. Technol., 3 (2013) 152-160.
[42] H. Li, C.L. Stern, T.J. Marks, Macromolecules, 38 (2005) 9015-9027.
[43] L. Resconi, L. Cavallo, A. Fait, F. Piemontesi, Chem. Rev., 100 (2000) 1253-1346.
[44] M.C. Baier, M.A. Zuideveld, S. Mecking, Angew. Chem. Int. Ed., 53 (2014) 9722-9744.

[45] Y. Gao, A.R. Mouat, A. Motta, A. Macchioni, C. Zuccaccia, M. Delferro, T.J. Marks, ACS Catal., 5 (2015) 5272-5282.
[46] T.R. Younkin, E.F. Connor, J.I. Henderson, S.K. Friedrich, R.H. Grubbs, D.A. Bansleben, Science, 287 (2000) 460-462.
[47] F.-S. Liu, H.-B. Hu, Y. Xu, L.-H. Guo, S.-B. Zai, K.-M. Song, H.-Y. Gao, L. Zhang, F.-M. Zhu, Q. Wu, Macromolecules, 42 (2009) 7789-7796.
[48] Q. Mahmood, Y. Zeng, X. Wang, Y. Sun, W.H. Sun, Dalton Trans., 46 (2017) 6934-6947.
[49] E. Yue, Y. Zeng, W. Zhang, F. Huang, X.-P. Cao, T. Liang, W.-H. Sun, Inorg. Chim. Acta, 442 (2016) 178-186.
[50] Fang Huang, Wenjuan Zhang, Yang Sun, Xinquan Hu, G.A. Solan, W.-H. Sun, New J. Chem., 40 (2016) 8012-8023.
[51] M.P. Weberski, C. Chen, M. Delferro, C. Zuccaccia, A. Macchioni, T.J. Marks, Organometallics, 31 (2012) 3773-3789.
[52] J. Wang, E. Yao, Z. Chen, Y. Ma, Macromolecules, 48 (2015) 5504-5510.
[53] Z. Cai, D. Xiao, L.H. Do, J. Am. Chem. Soc., 137 (2015) 15501-15510.
[54] M.R. Radlauer, M.W. Day, T. Agapie, J. Am. Chem. Soc., 134 (2012) 1478-1481.
[55] M.R. Radlauer, M.W. Day, T. Agapie, Organometallics, 31 (2012) 2231-2243.
[56] M.R. Radlauer, A.K. Buckley, L.M. Henling, T. Agapie, J. Am. Chem. Soc., 135 (2013) 3784-3787.
[57] C.M. Killian, D.J. Tempel, L.K. Johnson, M. Brookhart, J. Am. Chem. Soc., 118 (1996) 11664-11665.
[58] B.A. Rodriguez, M. Delferro, T.J. Marks, Organometallics, 27 (2008) 2166-2168.
[59] B.A. Rodriguez, M. Delferro, T.J. Marks, J. Am. Chem. Soc., 131 (2009) 5902-5919.
[60] M.P. Weberski, C. Chen, M. Delferro, T.J. Marks, Chem. Eur. J., 18 (2012) 10715-10732.
[61] T. Hu, L.-M. Tang, X.-F. Li, Y.-S. Li, N.-H. Hu, Organometallics, 24 (2005) 2628-2632.
[62] W.-H. Wang, G.-X. Jin, Inorg. Chem. Commun., 9 (2006) 548-550.
[63] D. Zhang, G.-X. Jin, Inorg. Chem. Commun., 9 (2006) 1322-1325.
[64] T. Hu, Y.-G. Li, Y.-S. Li, N.-H. Hu, J. Mol. Catal. A: Chem., 253 (2006) 155-164.
[65] Q. Chen, J. Yu, J. Huang, Organometallics, 26 (2007) 617-625.
[66] P. Wehrmann, S. Mecking, Organometallics, 27 (2008) 1399-1408.
[67] S.J. Na, D.J. Joe, S. S, W.-S. Han, S.O. Kang, B.Y. Lee, J. Organomet. Chem., 691 (2006) 611-620.
[68] D. Takeuchi, Y. Chiba, S. Takano, K. Osakada, Angew. Chem. Int. Ed., 52 (2013) 12536-12540.
[69] D.V. Soldatov, A.T. Henegouwen, G.D. Enright, C.I. Ratcliffe, J.A. Ripmeester, Inorg. Chem., 40 (2001) 1626-1636.
[70] M.D. Brandon A. Rodriguez, T.J. Marks, J. Am. Chem. Soc., 135 (2013) 17651.
[71] D. Guironnet, T. Friedberger, S. Mecking, Dalton Trans., (2009) 8929-8934.
[72] R. Robson, Inorg. Nucl. Chem. Lett., 6 (1970) 125-128.
[73] R. Wang, X. Sui, W. Pang, C. Chen, ChemCatChem, 8 (2016) 434-440.
[74] C. Rong, F. Wang, W. Li, M. Chen, Organometallics, 36 (2017) 4458-4464.
[75] S. Jie, D. Zhang, T. Zhang, W.-H. Sun, J. Chen, Q. Ren, D. Liu, G. Zheng, W. Chen, J. Organomet. Chem., 690 (2005) 1739-1749.

[76] S. Kong, K. Song, T. Liang, C.Y. Guo, W.H. Sun, C. Redshaw, Dalton Trans., 42 (2013) 9176-9187.
[77] Q. Xing, K. Song, T. Liang, Q. Liu, W.H. Sun, C. Redshaw, Dalton Trans., 43 (2014) 7830-7837.
[78] Y. Cui, S. Zhang, W.-h. Sun, Chin. J. Polym. Sci., 26 (2008).
[79] Y.-N. Zeng, Q.-F. Xing, Y.-P. Ma, W.-H. Sun, Chin. J. Polym. Sci., 36 (2018) 207-213.
[80] H. Liu, W. Zhao, X. Hao, C. Redshaw, W. Huang, W.-H. Sun, Organometallics, 30 (2011) 2418-2424.
[81] Y.D.M. Champouret, J. Fawcett, W.J. Nodes, K. Singh, G.A. Solan, Inorg. Chem., 45 (2006) 9890-9900.
[82] J.D.A. Pelletier, J. Fawcett, K. Singh, G.A. Solan, J. Organomet. Chem., 693 (2008) 2723-2731.
[83] C. Bianchini, G. Giambastiani, I.G. Rios, A. Meli, W. Oberhauser, L. Sorace, A. Toti, Organometallics, 26 (2007) 5066-5078.
[84] P. Barbaro, C. Bianchini, G. Giambastiani, I.G. Rios, A. Meli, W. Oberhauser, A.M. Segarra, L. Sorace, A. Toti, Organometallics, 26 (2007) 4639-4651.
[85] S. Zhang, W.-H. Sun, X. Kuang, I. Vystorop, J. Yi, J. Organomet. Chem., 692 (2007) 5307-5316.
[86] S. Zhang, I. Vystorop, Z. Tang, W.-H. Sun, Organometallics, 26 (2007) 2456-2460.
[87] (a) A.P. Armitage, Y. D. M. Champouret, H. Grigoli, J. D. A. Pelletier, K. Singh, G.A. Solan, Eur. J. Inorg. Chem., 2008 (2008) 4597-4607; (b) G. A. Solan, J. D. A. Pelletier, WO2005/118605(A1), December 15, 2005; (c) Q. Khamker, Y. D. M. Champouret, K. Singh, G. A. Solan, Dalton Trans., 41 (2009) 8935-8944; (d) Y. D. M. Champouret, J.-D. Marechal, I. Dadhiwala, J. Fawcett, D. Palmer, K, singh, G. A. Solan, Dalton Trans., 19 (2006) 2350-2361; (e) N. Savjani, K. Singh, G. A. Solan, Inorg. Chim. Acta, 436 (2015) 184-194.
[88] W.-H. Sun, Q. Xing, J. Yu, E. Novikova, W. Zhao, X. Tang, T. Liang, C. Redshaw, Organometallics, 32 (2013) 2309-2318.
[89] L. Wang, J. Sun, Inorg. Chim. Acta, 361 (2008) 1843-1849.
[90] Q. Xing, T. Zhao, S. Du, W. Yang, T. Liang, C. Redshaw, W.-H. Sun, Organometallics, 33 (2014) 1382-1388.
[91] Q. Xing, T. Zhao, Y. Qiao, L. Wang, C. Redshaw, W.-H. Sun, RSC Adv., 3 (2013) 26184-26193.
[92] Q. Chen, W. Zhang, G.A. Solan, T. Liang, W.H. Sun, Dalton Trans., 47 (2018) 6124-6133.
[93] D. Takeuchi, S. Takano, Y. Takeuchi, K. Osakada, Organometallics, 33 (2014) 5316-5323.
[94] C. Bianchini, G. Mantovani, A. Meli, F. Migliacci, F. Zanobini, F. Laschi, A. Sommazzi, Eur. J. Inorg. Chem., 2003 (2003) 1620-1631.
[95] G.J.P. Britovsek, M. Bruce, V.C. Gibson, B.S. Kimberley, P.J. Maddox, S. Mastroianni, S.J. McTavish, C. Redshaw, G.A. Solan, S. Strömberg, A.J.P. White, D.J. Williams, J. Am. Chem. Soc., 121 (1999) 8728-8740.
[96] J. Yu, H. Liu, W. Zhang, X. Hao, W.H. Sun, Chem. Commun., 47 (2011) 3257-3259.
[97] G.P. Abramo, L. Li, T.J. Marks, J. Am. Chem. Soc., 124 (2002) 13966-13967.
[98] J. Kuwabara, D. Takeuchi, K. Osakada, Chem. Commun., (2006) 3815-3817.
[99] M. Tanabiki, K. Tsuchiya, Y. Motoyama, H. Nagashima, Chem. Commun., (2005) 3409-3411.
[100] T. Sun, Q. Wang, Z. Fan, Polymer, 51 (2010) 3091-3098.
[101] S. Zhang, Q. Xing, W.-H. Sun, RSC Adv., 6 (2016) 72170-72176.